

# Paleoceanography and Paleoclimatology



## RESEARCH ARTICLE

10.1029/2018PA003459

### Key Points:

- Enhanced river runoff from northern borderlands occurs during sapropel S1
- Progressive water depth-related changes in redox conditions, ranging from sulfidic in early- to nearly oxic in last phase of S1
- There is Synchronous basin-wide initiation but possibly with progressively downward ventilation of bottom waters at ending of S1

### Supporting Information:

- Supporting Information S1

### Correspondence to:

A. Filippidi,  
a.filippidi@uu.nl

### Citation:

Filippidi, A., & De Lange, G. J. (2019). Eastern Mediterranean deep water formation during sapropel S1: A reconstruction using geochemical records along a bathymetric transect in the Adriatic outflow region. *Paleoceanography and Paleoclimatology*, 34, 409–429. <https://doi.org/10.1029/2018PA003459>

Received 9 AUG 2018

Accepted 27 FEB 2019

Accepted article online 04 MAR 2019

Published online 28 MAR 2019

## Eastern Mediterranean Deep Water Formation During Sapropel S1: A Reconstruction Using Geochemical Records Along a Bathymetric Transect in the Adriatic Outflow Region

A. Filippidi<sup>1</sup> and G. J. De Lange<sup>1</sup>

<sup>1</sup>Department of Earth Sciences-Geochemistry, Faculty of Geosciences, Utrecht University, Utrecht, The Netherlands

**Abstract** Eastern Mediterranean thermohaline circulation is directly influenced by middle- and low-latitude climate systems. The dramatic paleoclimate changes during the last African Humid Period (~10–6 ka BP) were captured in Mediterranean sediments as the distinctly organic-rich unit sapropel S1. Here, deepwater formation variability during S1 deposition is reconstructed. We use geochemical records of three cores along a bathymetric transect (775-, 1,359-, and 1,908-m water depths), at the transition between the Adriatic DW-formation area and the Eastern Mediterranean. In all three cores, sedimentation rates are distinctly higher during S1, corresponding with enhanced runoff emanating from the Adriatic hinterland. Hence, major runoff did not only come from southern but also from northern borderlands in this period. During sapropel formation, enhanced levels of primary productivity occurred in the surface waters and oxygen-depleted conditions in the bottom waters for all sites. Conditions for sediment and bottom-water below ~1.4 km water depth were sulfidic throughout S1, but for intermediate depth (775 m) were anoxic only during the first part (S1a). Bottom-water oxygenation interrupted S1 formation at water depths down to ~1.4 km, during two brief episodes, at 8.2 and 7.4 cal. ka BP. From the 7.4 cal. ka BP ventilation onward, the transition to more oxygenated bottom-water conditions was more progressive for the intermediate water depth site (775 m) than for the deeper sites. Conditions remained fully oxic for all water depths following the S1-MarkerBed ventilation event. Possibly, the onset of continuously oxic conditions started slightly earlier at intermediate depth (775 m;  $6.6 \pm 0.3$  cal. ka BP) than at greater depths (1,359 m, 1,908 m;  $6.0 \pm 0.3$  cal. ka BP).

### 1. Introduction

The density-driven present-day deep water circulation in the Mediterranean renders the basin into a well-ventilated, oligotrophic ocean. Eastern Mediterranean climate conditions are dominated by dry summers and relatively cold winters (Malanotte-Rizzoli et al., 1999; Ozsoy et al., 1991; Robinson et al., 1992; Theocharis, 2009; Wu & Haines, 1996). The Atlantic surface water enters the Mediterranean through the Strait of Gibraltar and flows eastward with increasing salinity due to excess evaporation. In the Levantine basin it transforms to the Levantine Intermediate Water (Robinson et al., 1992; Wu et al., 2000) that acts as a prerequisite for deepwater formation (DW-formation; Lascaratos, 1993; Wu & Haines, 1996). In the present day, persistent cold northerly winds acting upon Adriatic and Aegean marginal seas during winter, result in DW-formation and the consequent oxygenation of bottom waters in the present-day Eastern Mediterranean basin (Canals et al., 2009; Pinardi & Masetti, 2000; Poulos et al., 1997; Schlitzer et al., 1991; Theocharis et al., 1993; Theocharis & Georgopoulos, 1993).

#### 1.1. Periods of Confined Ocean Circulation—Sapropel S1

The rhythmic formation of organic-rich units, named sapropels (Olauson, 1961), is the profound evidence of the repeatedly disrupted Eastern Mediterranean thermohaline circulation in response to orbitally induced climate perturbations (Hilgen, 1991; Rossignol-Strick, 1985). Specifically, these intervals reflect periods of more humid climate conditions for the circum-Mediterranean (Bout-Roumazeilles et al., 2013; Combourieu-Nebout et al., 2013; Kallel et al., 1996; Magny et al., 2013; Siani et al., 2013) that further attest the basin's direct and indirect response to solar radiation related climate variability (Grant et al., 2016; Hennekam et al., 2014; Rossignol-Strick, 1985; Ziegler et al., 2010). The latter is associated with the

©2019. The Authors.

This is an open access article under the terms of the Creative Commons Attribution-NonCommercial-NoDerivs License, which permits use and distribution in any medium, provided the original work is properly cited, the use is non-commercial and no modifications or adaptations are made.

position of the Intertropical Convergence Zone (ITCZ) and monsoonal intensity, hence arid/humid conditions in North Africa, which in turn are closely linked to the Mediterranean water circulation, hence DW-formation.

The most recent sapropel S1, formed in the Eastern Mediterranean between ~10.8 and 6.1 cal. ka BP (de Lange et al., 2008). Its deposition has taken place during the African Humid Period (de Menocal et al., 2000), when intense humid climate conditions prevailed in the entire area, related to minimal precession/maximal insolation (Hilgen, 1991; Lourens, 2004; Rossignol-Strick, 1985). The enhanced Nile and other rivers runoff is thought to have resulted not only in a reduced salinity but possibly in enhanced primary production for the surface waters (Calvert, 1983; Calvert & Fontugne, 1987; Calvert & Pedersen, 1993; De Lange & Ten Haven, 1983; Meyer & Kump, 2008). The reduced salinity as well as sea level rise (Grant et al., 2016) are thought to have led to the weakening of Levantine Intermediate Water formation. All hydrological changes resulted in the basin-wide water column to become stratified, shoaling of the pycnocline and nutricline (e.g., Ariztegui et al., 2000; Castradori, 1993; Rohling, 1991; Rohling & Gieskes, 1989; Sachs & Repeta, 1999; Tesi et al., 2017) and ceased DW-formation. As a consequence, high primary production and depleted deep water oxygen conditions resulted in enhanced preservation of sedimentary organic matter (De Lange & Ten Haven, 1983; De Lange et al., 2008; Möbius et al., 2010; Moodley et al., 2005; Murat & Got, 2000; Olauson, 1961).

## 1.2. Sediment and Water Column Properties During Sapropel Formation

The distinct geochemical signature of a sapropel unit reflects sediment and water column environmental conditions during its formation. Elevated TOC(%) (Total Organic Carbon) in comparison to the enclosing marls confirms the increased flux and preservation of organic matter, which in combination with the enhanced Ba/Al ratios points to enhanced primary production in the surface waters (De Lange et al., 1989; Dymond et al., 1992; Martinez-Ruiz et al., 2000; Van Os et al., 1991).

Anoxic to sulfidic conditions are thought to have been consistently established at greater depths and at least intermittently, at intermediate and shallow water depths (Arnaboldi & Meyers, 2007; Gallego-Torres et al., 2010; Nijenhuis et al., 1999). Enrichments of elements such as V, Mo, Fe, and S are attributed to the formation of sulfide phases such as pyrite, or to their reduction to other insoluble forms (Brumsack, 1989; Calvert, 1983; Crusius et al., 1996; Jilbert et al., 2010; Mercone et al., 2001; Pruyssers et al., 1991; Warning & Brumsack, 2000). Vanadium is associated to suboxic conditions and organic matter (Emerson & Husteded, 1991; Rutten & De Lange, 2003), whereas Mo, Fe, and S require completely anoxic and sulfidic conditions in order to be retained in the sediments.

In contrast, manganese is predominantly present in the form of oxides, whereas at low-oxygen conditions, it readily serves as an electron donor for the microbial degradation of organic matter and is removed from the sediments as dissolved  $Mn^{2+}$  (De Lange, 1986; De Lange et al., 1994; Froelich et al., 1979; Mangini et al., 1990). Therefore, Mn/Al profiles can be used to describe the redox state of sediments and overlying water.

The dissolved  $Mn^{2+}$  is transported laterally and also upward to shallower depths where it may form oxides once again at the redoxcline in the sediment and in the water column. Upon reventilation, the high levels of dissolved manganese promptly form oxides that precipitate, resulting in prominent enhancements in manganese concentrations in sedimentary profiles (e.g., De Lange et al., 1989, 1994; Mangini et al., 1990; Reitz et al., 2006; Thomson et al., 1999). Consequently, the end of sapropel formation and resumption of more continuous DW ventilation is manifested by the distinctly Mn-rich, dark layer, “Marker Bed” (Ariztegui et al., 2000; Cita et al., 1989; De Lange et al., 1989, 2008; Thomson et al., 1995; van Santvoort et al., 1996).

However, in many cases, the primary geochemical composition of the sediment has been altered by syndepositional and postdepositional processes (e.g., De Lange et al., 1989; Passier et al., 1996; Passier & De Lange, 1998; Prahl et al., 1989; Thomson et al., 1999; van Santvoort et al., 1996; Wilson et al., 1985). The former process is developed during sapropel formation, due to downward diffusing dissolved sulfide that resulted in the progressive downward sulfidization of available Fe in the underlying sediments, thus forming a pyrite-rich zone beneath the sapropel layer (Passier et al., 1996, 1997, 1999; Passier & De Lange, 1998). Its development merely signifies intense excess sulfide production during sapropel formation within sapropel sediments and its transport toward bottom water and underlying sediments. Another diagenetic feature often observed in

the upper part of sapropel units is the development of an oxidation front, which starts upon the reventilation of bottom waters at the end of sapropel formation. Penetration of oxygen into the sediment results in the downward progressing oxidation of organic matter and pyrite (De Lange et al., 1989, 1994, 2008; Pruyssers et al., 1993; Thomson et al., 1995; van Santvoort et al., 1996). This process is commonly indicated by a second peak in Mn/Al, below the Mn/Al ventilation peak (Marker Bed), whereas it affects not only the distribution of TOC(%) and organic biomarkers (Versteegh et al., 2010) but also the distribution of redox-sensitive elements and that of Fe and S due to pyrite oxidation.

### 1.3. Variability During S1 Formation

During S1 formation, the circulation in the Mediterranean, albeit diminished, maintained its current anticyclonic configuration (Myers et al., 1998; Nijenhuis et al., 1999; Rohling, 1994; Stratford et al., 2000). However, the intermediate water mass was suggested to be restricted to the top few hundred meters (Rohling, 1991), whereas the water column at greater depths was mostly anoxic or even sulfidic (Passier et al., 1996, 1997; Reed et al., 2011). Recent studies have indicated that sapropel deposition may not have occurred exclusively under permanently anoxic conditions (Casford et al., 2003; Siani et al., 2013) at least not for shallower depths (Filippidi et al., 2016). The sporadic renewal of the water column at intermediate water depths has been suggested (Casford et al., 2003; Rohling et al., 2015; Tachikawa et al., 2015), which could explain a continuous supply of riverine and oceanic-derived trace metals to these levels (Nijenhuis et al., 1999). In addition, distinct major sapropel interruption events have been reported for 8.2 and 7.4 cal. ka BP (e.g., Ariztegui et al., 2000; Filippidi et al., 2016; Rohling et al., 1997; Triantaphyllou et al., 2016). The first interruption event is thought to be the result of a cold northern borderland episode that has caused the cooling of surface waters and the subsequent temporary resumption of DW-formation (Alley et al., 1997; Bar-Matthews et al., 1999; De Rijk et al., 1999; Kotthoff et al., 2008; Marino et al., 2009; Pross et al., 2009; Rohling et al., 1997; Rohling & Pälike, 2005). Thereafter, warm and humid conditions reinstated in the basin area; hence, sapropel formation resumed. The second cold episode, at 7.4 ka BP, prominently expressed in a number of marine and terrestrial records coincides with a northerly cold outbreak and the beginning of the gradual retreat of the ITCZ and thus the weakening of humid conditions. This event also triggered the resumption of DW overturning at intermediate water depth (~700 m), temporarily in the Adriatic Sea and more permanently in the Aegean Sea (Filippidi et al., 2016; Goudeau et al., 2014; Kouli et al., 2012; Triantaphyllou et al., 2016). Consequently, the wide range of sapropel S1 deposits studied throughout the Eastern Mediterranean basin have revealed that sapropel formation has taken place under variable depositional settings. These include different water depths, regional and sedimentary conditions as well as sediment accumulation rates. Redox sedimentary conditions are crucial for the preservation of marine archives; hence, the availability of oxygen at the sea bottom plays a pivotal role, which in turn is controlled by the DW overturn and organic matter fluxes.

In this study, we focus on three cores retrieved from a bathymetric transect (775, 1,359, and 1,908 m) of a site under the direct influence of DW-formation from the South Adriatic Sea and with relatively high sedimentation rates. The Adriatic Sea is the primary deep water source for the Eastern Mediterranean; hence, hydrological changes related to DW-formation are expected to be captured in the sedimentary record of the studied cores. Since the three cores are from the same site, primary composition is expected to be similar and hence differences are expected to reflect differences in DW-formation and related redox conditions that developed during S1 formation, at different water depths. The water depths selected are thought to be diagnostic for processes occurring in key water masses: shallow-intermediate water depth (775 m), transitional water depth (1,359 m), and deepwater (1,908 m; Malanotte-Rizzoli et al., 1997). Therefore, with this comparison, we aim to determine variability in hydrological conditions during S1 formation, (recurrent) ventilation and DW-formation in relation to climate conditions, and the consequent variability in preservation potential.

To this end, we first assess S1 sapropel boundaries for the sediments in our cores taking into account potential post-depositional alteration so as to distinctly recognize primary signals. Subsequently, primary productivity and preservation are compared to depositional setting along a bathymetric transect. This permits us to provide an integrated picture of sequential changes in depth of deepwater ventilation and the associated formation and preservation of sedimentary sapropel units as related to global climate.

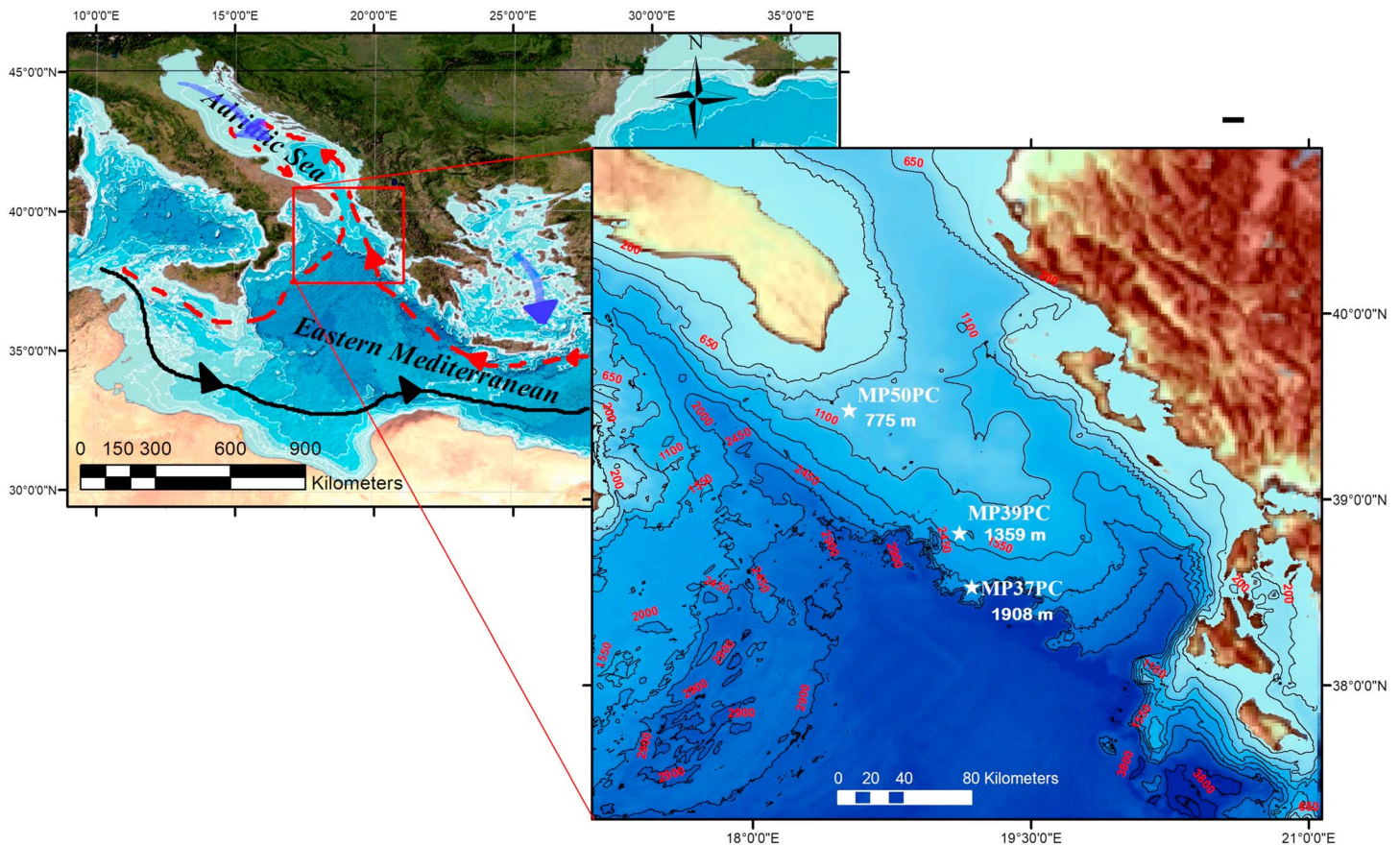


**Figure 1.** (left) Map of the Eastern Mediterranean Sea. Red square indicates the study area. (right) Bathymetric map with the location of the three studied cores MP50-MP39-MP37PC at 775-, 1,359-, and 1,908-m water depths, respectively. Information contained here has been derived from data that are made available under the European Marine Observation Data Network Seabed Habitats project (<http://www.emodnet-seabedhabitats.eu/>), funded by the European Commission's Directorate-General for Maritime Affairs and Fisheries. Black, red, and blue lines and arrows depict surface, (Levantine) intermediate, and deep water circulation pattern, respectively.

## 2. Material and Methods

### 2.1. Material

In this study, three piston cores, retrieved during the Macchiato 2009 cruise with RV *Pelagia* from sites immediately south of the western Otranto Strait sill (South Adriatic Sea), are used. These sites extend along a NW-SE bathymetric transect: MP50PC (39°N29', 18°E31', total length 4.75 m), MP39PC (38°N49.18', 19°E6.8', total length 6.7 m), and MP37PC (38°N31.81', 19°E10.84', total length 6 m) and at water depths of 775, 1,359, and 1,908 m, respectively (Figure 1 and Table 1). All three cores were sampled at 0.5-cm resolution.

### 2.2. Methods

Samples were divided into two aliquots, for micropaleontological and for geochemical analyses. For the latter, samples were freeze-dried and ground with an agate mortar.

#### 2.2.1. Organic C

The organic carbon content was measured with a Fisons NA1500 CNS elemental analyzer using samples decarbonated with 1 M HCl (4 and 12 hr; cf. Wu et al., 2017). The average standard deviation for international and laboratory standards was better than 1%.

#### 2.3. $\delta^{18}\text{O}$ Composition

Three fractions (350, 125, and 63  $\mu\text{m}$ ) were used for wet sieving and then dried at 40 °C. On average, 25 *Globigerinoides ruber* s.s. white were handpicked after dry sieving, from 250- to 200- $\mu\text{m}$  size fraction, crushed

**Table 1**  
Carbon-14 Dated Points and  $1\sigma$  Calibrated Ages (ka)

Sample	Lab code	Average depth	$^{14}\text{C}$ age	$\Delta R$	$1\sigma$ age	Age (cal. ka BP)
a: MP50PC#5 5,0–5,5	Poz-51750	5.2	3700 $\pm$ 30 BP	118 $\pm$ 60	3366–3738	3.55 $\pm$ 0.2
b: MP50PC#5 19,5–20,0	Poz-51746	19.7	6265 $\pm$ 35 BP	118 $\pm$ 60	6481–6866	6.69 $\pm$ 0.2
c: MP50PC#5 39,0–39,5	Poz-51748	39.2	8020 $\pm$ 40 BP	118 $\pm$ 60	8314–8703	8.51 $\pm$ 0.2
d: MP50PC#5 48,5–49,0	Poz-51749	48.7	8670 $\pm$ 50 BP	118 $\pm$ 60	9146–9559	9.35 $\pm$ 0.2
e: MP50PC#5 57,0–57,5	Poz-51752	57.2	9540 $\pm$ 50 BP	118 $\pm$ 60	10095–10644	10.36 $\pm$ 0.3
f: MP50PC#4 36,5–37,0	Poz-51745	111.7	17930 $\pm$ 90 BP	118 $\pm$ 60	19920–21730	21.0 $\pm$ 0.9
g: MP39PC#7 7,0–7,5	Poz-63677	7.25	2325 $\pm$ 30 BP	118 $\pm$ 60	1597–1989	1.8 $\pm$ 0.2
h: MP39PC#7 20,5–21,0	Poz-63678	20.75	4810 $\pm$ 30 BP	118 $\pm$ 60	4621–5223	4.9 $\pm$ 0.3
i: MP39PC#7 26,5–27,0	Poz-63679	26.75	5650 $\pm$ 30 BP	118 $\pm$ 60	5738–6235	5.99 $\pm$ 0.2
j: MP39PC#7 28,5–29,0	Poz-63680	28.75	5870 $\pm$ 30 BP	118 $\pm$ 60	6111–6377	6.25 $\pm$ 0.1
k: MP39PC#7 43,5–44,0	Poz-63681	43.75	8285 $\pm$ 35 BP	118 $\pm$ 60	8420–9037	8.72 $\pm$ 0.3
l: MP39PC#7 50,0–50,5	Poz-63682	50.25	9160 $\pm$ 40 BP	118 $\pm$ 60	9243–10147	9.71 $\pm$ 0.5
m: MP39PC#7 62,5–63,0	Poz-63683	62.75	12290 $\pm$ 50 BP	118 $\pm$ 60	12588–13847	13.2 $\pm$ 0.6
n: MP37PC#6 17,5–18,0	Poz-74669	17.75	3135 $\pm$ 30	118 $\pm$ 60	2608–3011	2.81 $\pm$ 0.2
o: MP37PC#6 30,0–30,5	Poz-63685	30.25	4620 $\pm$ 30 BP	118 $\pm$ 60	4256–4915	4.62 $\pm$ 0.3
p: MP37PC#6 40,0–40,5	Poz-63686	40.25	6480 $\pm$ 30 BP	118 $\pm$ 60	6490–7140	6.85 $\pm$ 0.3
q: MP37PC#6 50,0–50,5	Poz-63687	50.25	7775 $\pm$ 35 BP	118 $\pm$ 60	7900–8493	8.23 $\pm$ 0.3
r: MP37PC#6 61,0–61,5	Poz-63688	61.25	8860 $\pm$ 35 BP	118 $\pm$ 60	9078–9773	9.47 $\pm$ 0.3
s: MP37PC#6 66,0–66,5	Poz-81676	66.25	10040 $\pm$ 50 BP	118 $\pm$ 60	10213–10617	10.4 $\pm$ 0.2
t: MP37PC#6 72,0–72,5	Poz-63689	72.25	11540 $\pm$ 50 BP	118 $\pm$ 60	12209–12594	12.4 $\pm$ 0.2

Note.  $\Delta R$ : regional reservoir age.

and cleaned with Milli-Q water and put for 10 s in an ultrasonic bath. After drying, approximately 30  $\mu\text{g}$  was used for measuring the  $\delta^{18}\text{O}$  and  $\delta^{13}\text{C}$  composition in a Kiel device connected to a Finnigan MAT 253 IRMS. In-house and international standards were used (NBS-19), and the average standard deviation for all measurements was  $<0.1\%$ .

### 2.3.1. Elemental Composition

Elemental concentrations in the samples were determined using Perkin Optima 3000, an Inductively Coupled Plasma-Optical Emission Spectroscopy after total digestion in a HF,  $\text{HClO}_4$ , and  $\text{HNO}_3$  acid mix and subsequent dissolution in 1 M  $\text{HNO}_3$  (for details cf. Wu et al., 2018). The standard deviation for all measurements is better than 3%.

For minimizing variability due to carbonate dilution, that is, “closed-sum” effects, elemental concentrations are normalized to aluminum (Calvert & Pedersen, 1993; De Lange et al., 1987; Rinna et al., 2002; Wehausen & Brumsack, 1999).

Sedimentary  $\text{Fe}_{\text{tot}}$  is taken to be the sum of iron in (clay) minerals, iron oxides, and iron sulfide. Fe-sulfide in sapropels is predominantly pyrite ( $\text{FeS}_2$ ; Nijenhuis et al., 1999; Passier et al., 1996, 1997; Pruyssers et al., 1991). The average Fe/Al associated to (clay) minerals for this region is  $\sim 0.41$ . Although a slightly differing provenance may justify to use a slightly different ratio for different periods, we have chosen to use one ratio throughout. This may result in negative ratios (e.g., most distinctly for volcanic ash horizons). Thus, Fe (ox)/Al (%) was calculated using  $\text{Fe (ox)} = \text{Fe}_{\text{tot}} - 56/64 * \text{S}_{\text{tot}} - \text{Al} * 0.41$ . The  $\text{Fe}_{\text{tot}}/\text{Al}$  values are shown in the Supplementary Material (Figure S5 in the supporting information).

## 3. Results and Discussion

The three cores used in this study have been retrieved from the same area in a bathymetric transect. Hence, their primary composition related to surface water conditions and sediment provenance is expected to be similar. The study area is located south of Otranto Strait, in front of the Adriatic Deep Water Outflow (Canals et al., 2009; Cantoni et al., 2016; Langone et al., 2016). In this study, we aim to determine climate-induced variability in DW-formation and subsequent ocean circulation, and its imprint on marine sediments as related to water depth, during S1 deposition.

These sapropel intervals are characterized by enrichments in all cores for the Ba/Al ratio and in core MP50PC for the TOC(%). For the two deeper cores, the topmost part of S1 is affected by postdepositional

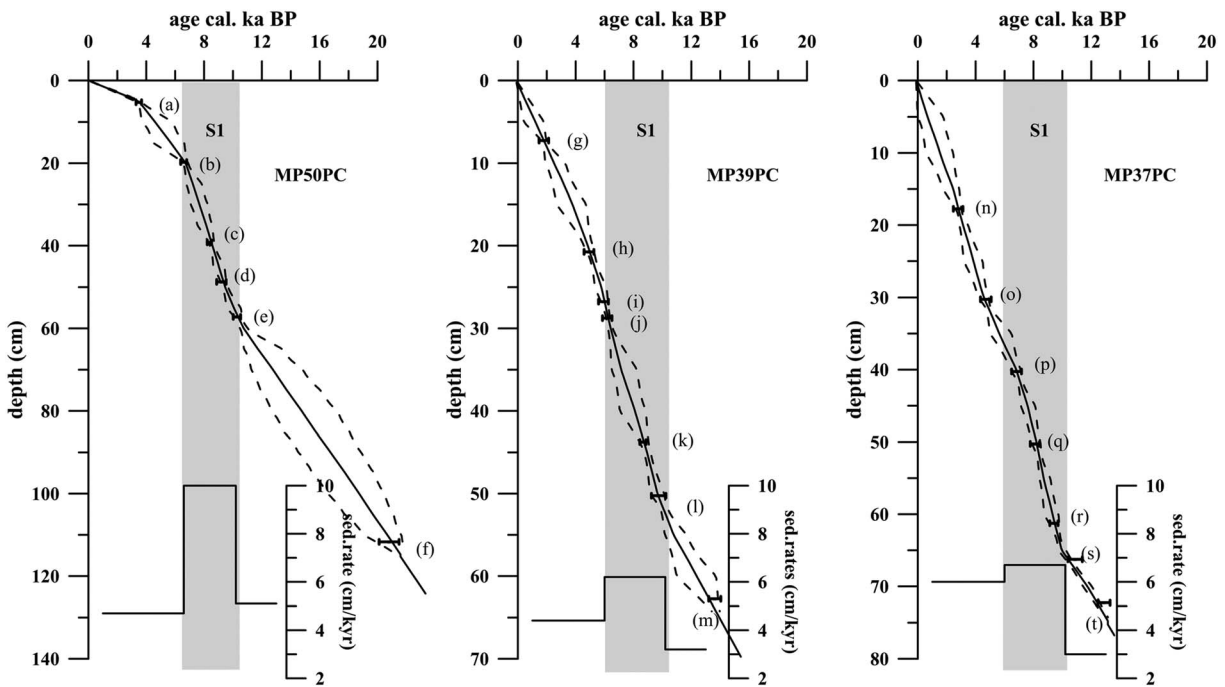


**Figure 2.** Age models for the three cores MP50PC, MP39PC, and MP37PC. Carbon-14 and calibrated ages (ka BP) are shown in Table 1 (points a–t). Gray shaded area indicates sapropel S1 period (after De Lange et al., 2008).

alternation. At the top of the Ba/Al enriched interval, a large Mn/Al peak is prominent at  $\sim 6.6 \pm 0.3$  cal. ka BP at the shallow site and at the other two sites (at  $\sim 6.0 \pm 0.3$  cal. ka BP).

The upper parts of all cores have a somewhat deviating composition due to the presence of volcanic ash layers and a possible nonsteady state depositional event for core MP50PC in particular. This is not relevant here as we focus on sediments older than 5 cal. ka BP, hence will no further be discussed.

### 3.1. Chronology and Sedimentation Rates

For the age model, 18 accelerator mass spectrometry radiocarbon  $^{14}\text{C}$  were done on clean, handpicked mixed planktonic foraminifera from the size fraction  $>63 \mu\text{m}$ , at Poznan Radiocarbon Laboratory (Poland). In addition,  $^{210}\text{Pb}$  contents were measured for the topmost sediments of all three cores (Table 1).

For the calibration of  $^{14}\text{C}$  dates, a regional reservoir age correction for the Adriatic Sea ( $\Delta R$ ) of  $118 \pm 30$  years was used (Reimer & McCormac, 2002; Siani et al., 2000). A Bayesian deposition model was applied for the probabilistic assessment of the age models, using Bacon software (Blaauw & Christen, 2011). Age-depth chronology is built by determining accumulation rates, whereas Markov Chain Monte Carlo method is used for the age estimation and a Student's  $t$  distribution with wide tails for the carbon dates (Figure 2; Blaauw & Christen, 2005; Blaauw & Christen, 2011; Christen & Perez, 2009; Ramsey, 2008). All ages will be discussed as calibrated years (cal. ka BP).

Consistent age versus depth profiles are observed for all cores, with age uncertainties varying between 0.4 and 1 ka within the S1 interval, and amounting up to 2 ka further below and above it (Figure 2). Dark colored S1 intervals occur from 19- to 55-cm depth in MP50PC, 24 to 51 cm in MP39PC, and 35 to 66.5 cm in MP37PC (supporting information Figure S2). Sedimentation rates during S1 are  $\sim 10$  cm/kyr for MP50PC,  $\sim 6.2$  cm/kyr for MP39PC, and  $\sim 6.7$  cm/kyr MP37PC. Postsapropel and presapropel sedimentation rates are much lower for all sites (Figure 2). For the topmost interval (i.e.,  $<5$  ka; top 15 cm) at the 775-m site (MP50PC), the derived sedimentation rate as well as deviating other features may refer to nonsteady state depositional processes. Here, we ignore this time interval and focus on the S1 interval for which the age framework is well constrained.

The tephra layer in core MP50PC, at  $\sim 9.3$  ka cal BP, with inferred provenance from E1 Gabelotto/Fiumebianco from Lipari Islands and Mercato Eruption from Sommas Vesuvius (D. Insinga

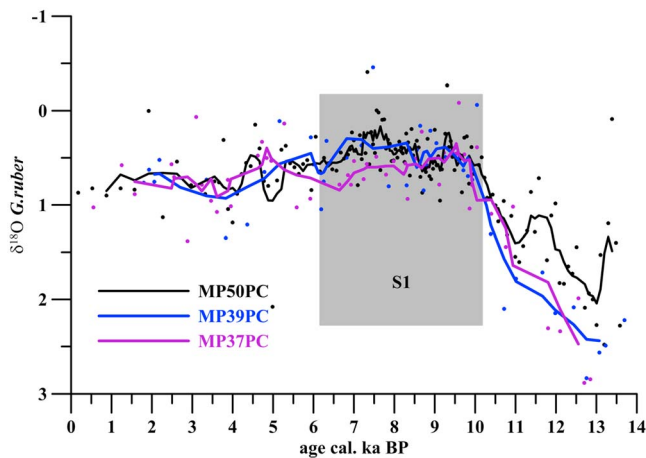


**Figure 3.**  $\delta^{18}\text{O}$  *Globigerinoides ruber* of the three cores MP50PC (black line), MP39PC (blue line), and MP37PC (purple line) confirming the robustness of the age models showing almost identical fluctuation (within the age error).

personal communication; July 9, 2014) having reported dates of  $8500 \pm 100$  cal. ka BP and  $9680 \pm 480$  cal. BP (Wulf et al., 2004, 2008), respectively. This confirms the accuracy of the age model (Figure S1 in the supporting information). Furthermore, independent proxies Ti/Al ratio of bulk sediment (Figure S1) and oxygen isotopic composition of *Globigerinoides ruber* s.s. white done in all three cores confirm the consistency of the age models within the  $^{14}\text{C}$  age uncertainty boundaries (Figure 3).

### 3.2. Humid Climate Conditions

The formation of sapropels is related to humid climate conditions that resulted not only in enhanced North African runoff but also in enhanced surface water productivity and water column stratification (Emeis et al., 2000, 2003; Marino et al., 2009; Rohling et al., 2004). This leads to reduced and ultimately ceased DW-formation and consequently to anoxic deep-water conditions, that is, organic matter preservation. The transition from fully ventilated to stagnant conditions is thought to take at least a few hundred years (Grimm et al., 2015; Schmiiedl et al., 2010). Thus, there may be considerable offset between proxies for humid climate (e.g., dust,

Ti/Al) and surface water salinity ( $\delta^{18}\text{O}_{\text{ruber}}$ ), and those for deepwater anoxia/preservation (i.e., TOC(%), Ba/Al, and trace elements). To evaluate such differences, the definition and objective assessment of exact boundaries is important. Therefore, we will first discuss boundaries and how these have been determined.

#### 3.2.1. Objectively Assessing Sapropel Boundaries

For the detailed evaluation of processes and sequence thereof, not only an accurate age model but also an objective methodology is needed to assess sapropel boundaries.

The interval during which sapropelic layers have been formed in all three cores is characterized by elevated Ba/Al ratios and TOC(%) contents (e.g., Pruyssers et al., 1991; Thomson et al., 1995; Van Santvoort et al., 1996; Warning & Brumsack, 2000; see section 1.2; Figures 4 and 5). Accordingly, the depth profiles for TOC(%) and Ba/Al are adequate for determining the sapropel onset (Figure S2 in the supporting information).

Geochemical proxies related to bottom-water and sediment anoxia cannot be used to determine the onset of sapropel conditions, due to downward sulfidization of the underlying sediments during sapropel formation (Passier et al., 1996, 1997). The latter process is reflected in the redox-sensitive elemental profiles at the two deeper sites in particular (see section 3.3.1; Figures 6 and 7). The Ba/Al ratio and organic carbon are not affected by this process, thus still represent initial conditions. Hence, we define the beginning of the sapropel using the abrupt onset of enhanced levels of TOC(%) and Ba/Al ratios that represent the elevated primary production in the surface waters and improved preservation at the seafloor due to diminished oxygen levels.

The sapropel ending is marked by a rapidly reduced Ba/Al and the Mn-reventilation peak (Marker Bed; Mn-MB from hereon; De Lange et al., 2008; for more details see supporting information Text S1). The TOC(%) can mostly not be used for the determination of the S1 upper boundary, due to postdepositional oxidation of the topmost part of the sapropel (see section 3.3.2; Figure 5). This is the case for cores MP39 and MP37, whereas for high sedimentation rate core MP50, such downward progressing oxidation does not seem to have taken place. Although the Ba/Al ratio in general is adequate to indicate sapropelic intervals, looking into more detail it seems that deviations occur. In particular, for cores MP37 and MP39 the Ba/Al level maintains at somewhat elevated values even after the end of the sapropel as defined by the Mn-MB. This seems directly related to the much-enhanced Mn/Al level of the Mn-MB and the associated slightly enhanced level of adsorbed Ba (De Lange et al., 1994; Reitz et al., 2006). In other words, the somewhat enhanced Ba/Al immediately above the sapropel upper boundary is related to Ba associated with large amounts of manganese oxides precipitation during the ventilation event. This is unrelated to typical sapropelic barite-Ba associated with enhanced organic matter fluxes to the seafloor. Hence, the exact upper boundary for the sapropel layer can best be defined using the Mn/Al ratio, that is, the Marker Bed (Mn-MB; see section 1.2 representing the reventilation/reoxygenation of bottom waters as a result of the resumption of DW-formation in the basin; Reitz et al., 2006; Van Santvoort et al., 1996). As the  $\text{MnO}_2$  in this Marker Bed is associated with

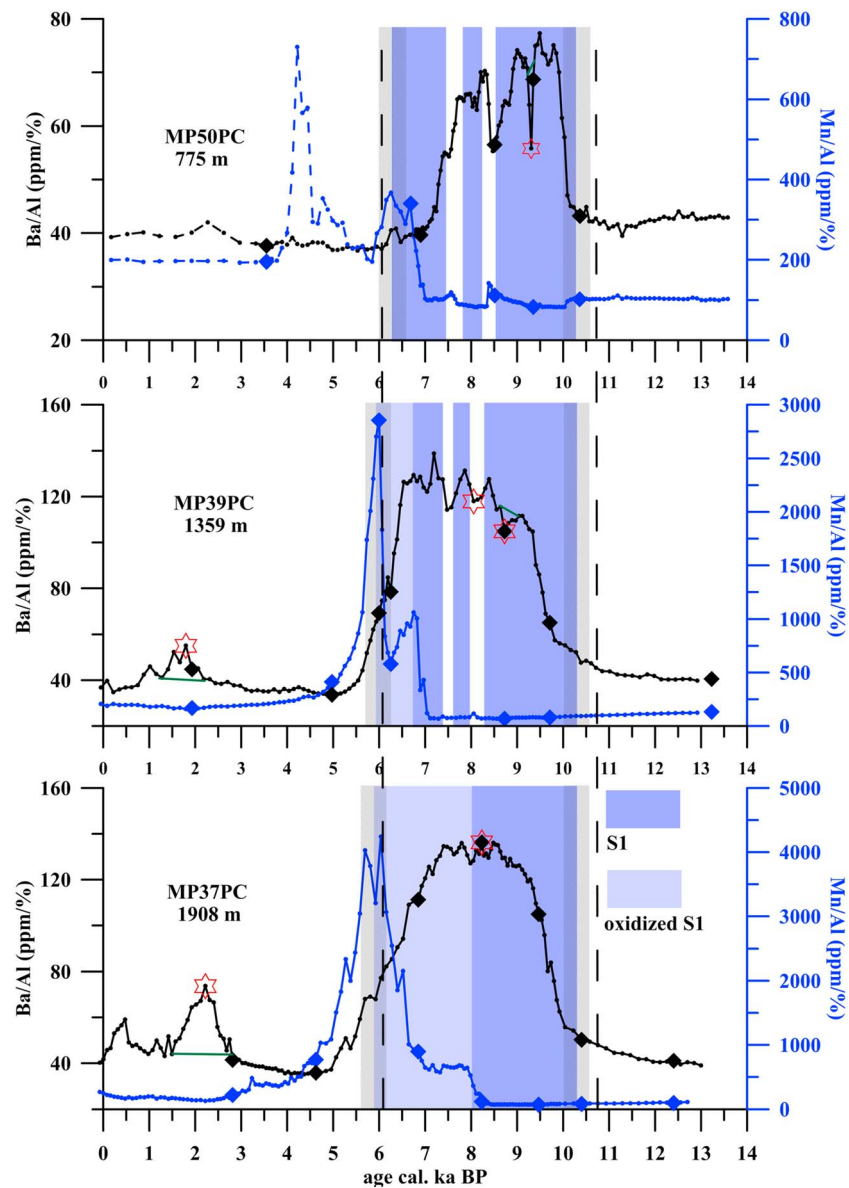


**Figure 4.** Elemental profiles: Ba/Al (ppm/%; black line) and Mn/Al (ppm/%; blue line) for the three cores. The most recent part in MP50PC core (<5 ka) is noted with a dashed line due to high age uncertainty. Filled diamonds show <sup>14</sup>C-dated samples and open red stars indicate samples with substantial volcanic ash. Green lines denote potential profile without tephra (i.e., 2-ka tephra has enhanced Ba/Al, whereas ~9-ka tephra has relatively reduced Ba/Al). Dark blue and light blue shaded areas indicate residual and oxidized S1 intervals, respectively. Hatched areas show sapropel upper and lower boundaries defined as explained in the supporting information (Figures S2 and S3 and Text S1). Vertical dashed black lines show the basin-wide sapropel boundaries by De Lange et al. (2008).

enhanced water column-derived adsorbed Mo, additional evidence for the depth of this event may be obtained using the Mo/Al ratio (Figure 6).

### 3.2.2. Enhanced Freshwater Supply From Northern Borderlands

The significantly higher sedimentation rates during S1 deposition are noticeable in all three cores. Within this interval, sedimentation rates are much higher compared to pre-S1 time (Figure 2). As the provenance of sediment in this region and in our cores is thought to be from the Adriatic area (Filippidi et al., 2016; Goudeau et al., 2013), this indicates the enhanced influx of fresh water from the Northern Borderlands. This intense runoff during the S1 period largely coincides with that for the southern borderlands, that is, during the Humid North African Period. Therefore, besides North African/River Nile discharge, which is

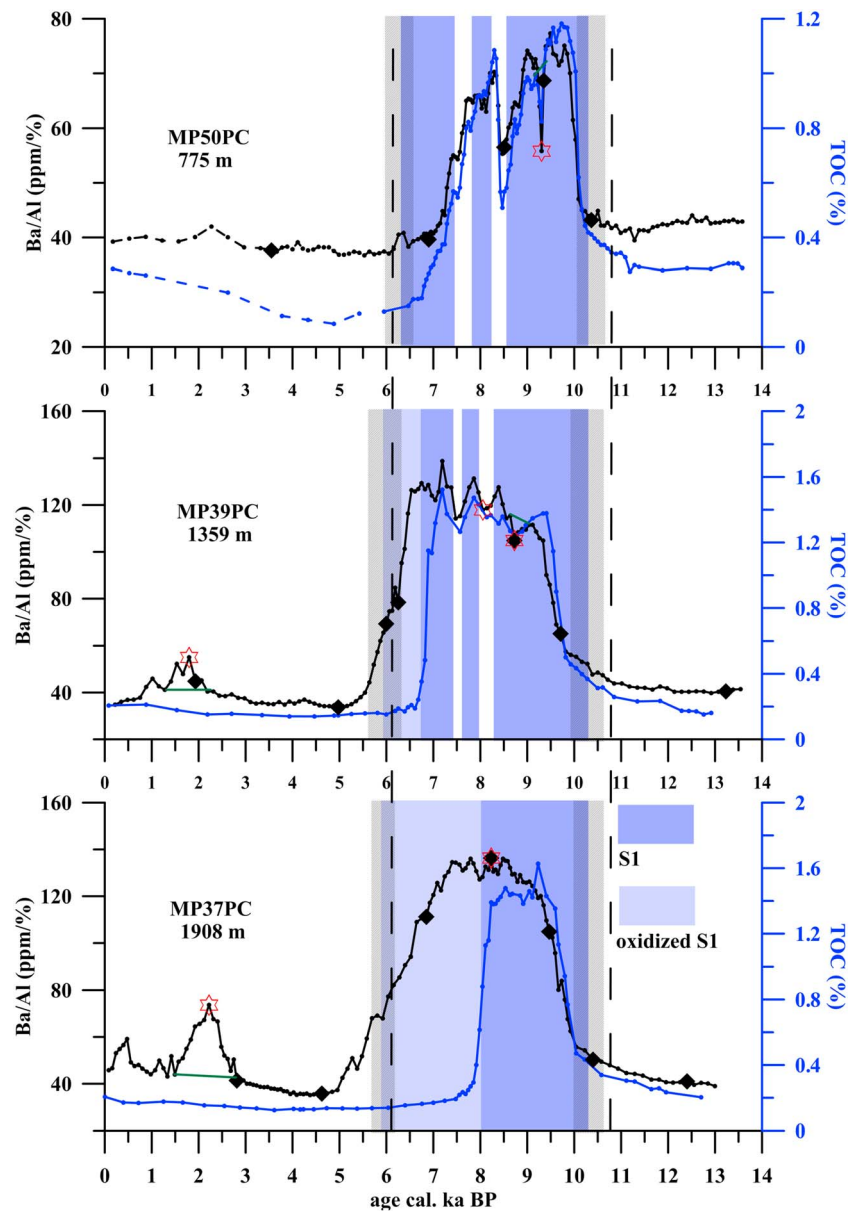


**Figure 5.** Elemental profiles: Ba/Al (ppm/%; black line) and TOC(%) (blue line) for the three cores. For dashed lines, green lines, symbols, and shading, see caption of Figure 4.

usually considered to be the most significant source of fresh water during S1, an additional enhanced freshwater discharge arrives from the northern borderlands. This is the first direct proof for such simultaneously occurring increased northern and southern borderlands runoff during sapropel S1. Such multiple-sourced runoff is reported to be required to reach a stagnant water column (Pinardi & Masetti, 2000).

### 3.3. Diagenetic Features

Before being able to evaluate primary sedimentary signals, we first need to assess potential diagenetic changes that may have affected the primary composition of the sediments. These are the syngenetic formation of a pyrite-rich *sulfidization zone* below the sapropel interval (Passier et al., 1996, 1997; Passier & De Lange, 1998; Reed et al., 2011) and the postdepositional *oxidation front* at the top of the sapropel (e.g., Pruyers et al., 1991; Reitz et al., 2006; Thomson et al., 1995; Van Santvoort et al., 1996).

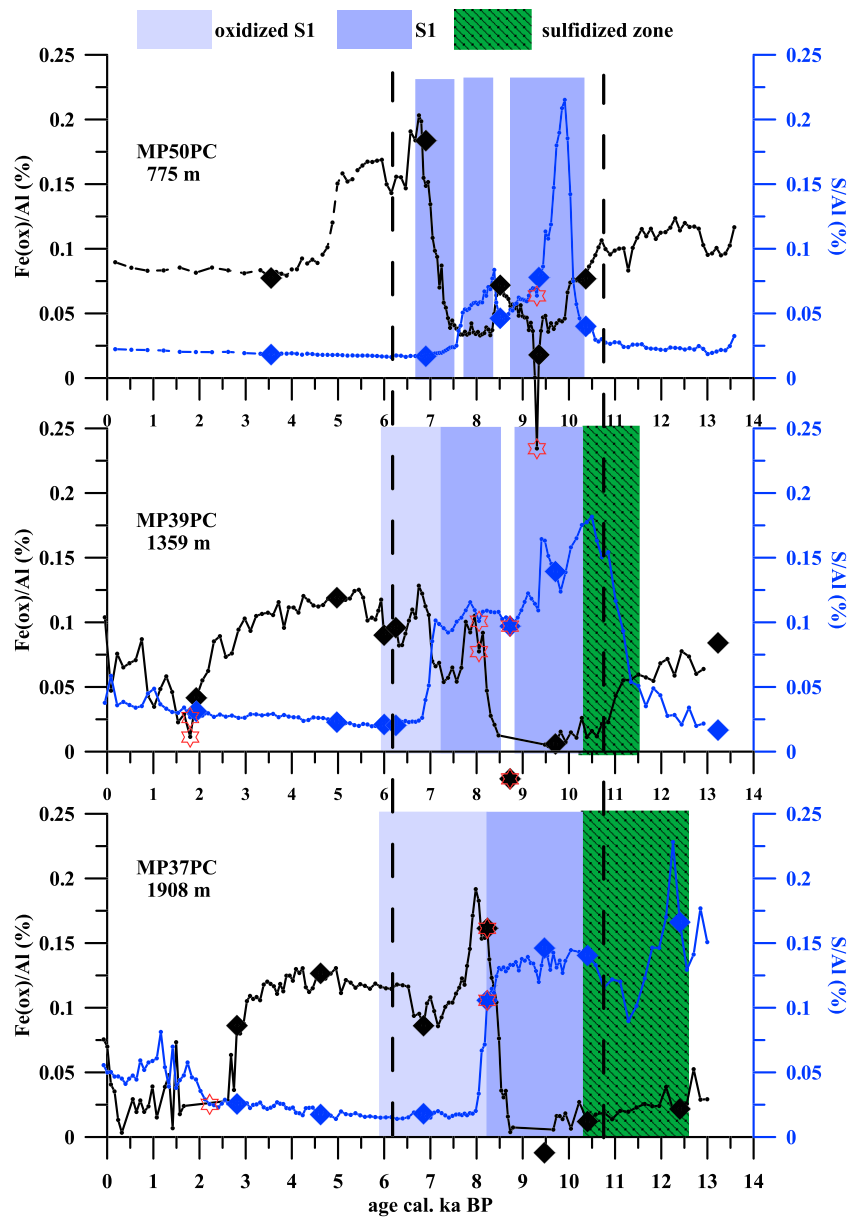


**Figure 6.** Elemental profiles V/Al (ppm/%; black line) and Mo/Al (ppm/%; blue line). Green shaded area indicates the sulfidization zone. Green lines denote potential profile without tephra (i.e., tephra has reduced V/Al). For dashed lines, symbols, and shading, see caption of Figure 4.

### 3.3.1. Sulfidization Zone

At the two deeper sites, that is, MP39PC and MP37PC, such a sulfidized zone has clearly developed immediately below the organic-rich interval, as indicated by diagnostic enrichments of Fe(ox)/Al and S/Al (Figure 7; Passier et al., 1996, 1999; Thomson et al., 1999). Furthermore, trace elements such as Mo have also been affected by the downward diffusion of sulfides and hence Mo/Al profiles appear enriched in this interval. In fact, the shape of Mo/Al profiles is identical to that of S/Al outlining the high affinity of Mo to S geochemistry (Figures 6 and 7). The sulfidized sediments extend to 10 and 15 cm below sapropel S1 in cores MP39 and MP37, at water depths of 1,359 and 1,908 m, respectively. The amount of reduced S below S1 is estimated to represent ~50% and 65% of the pyrite-S in the residual S1 interval, for MP39 and MP37 sites, respectively. Due to the relatively small sampling area, similar biological production rates in the surface waters are expected for all three cores; thus, any difference in sedimentary organic matter content must be related to different

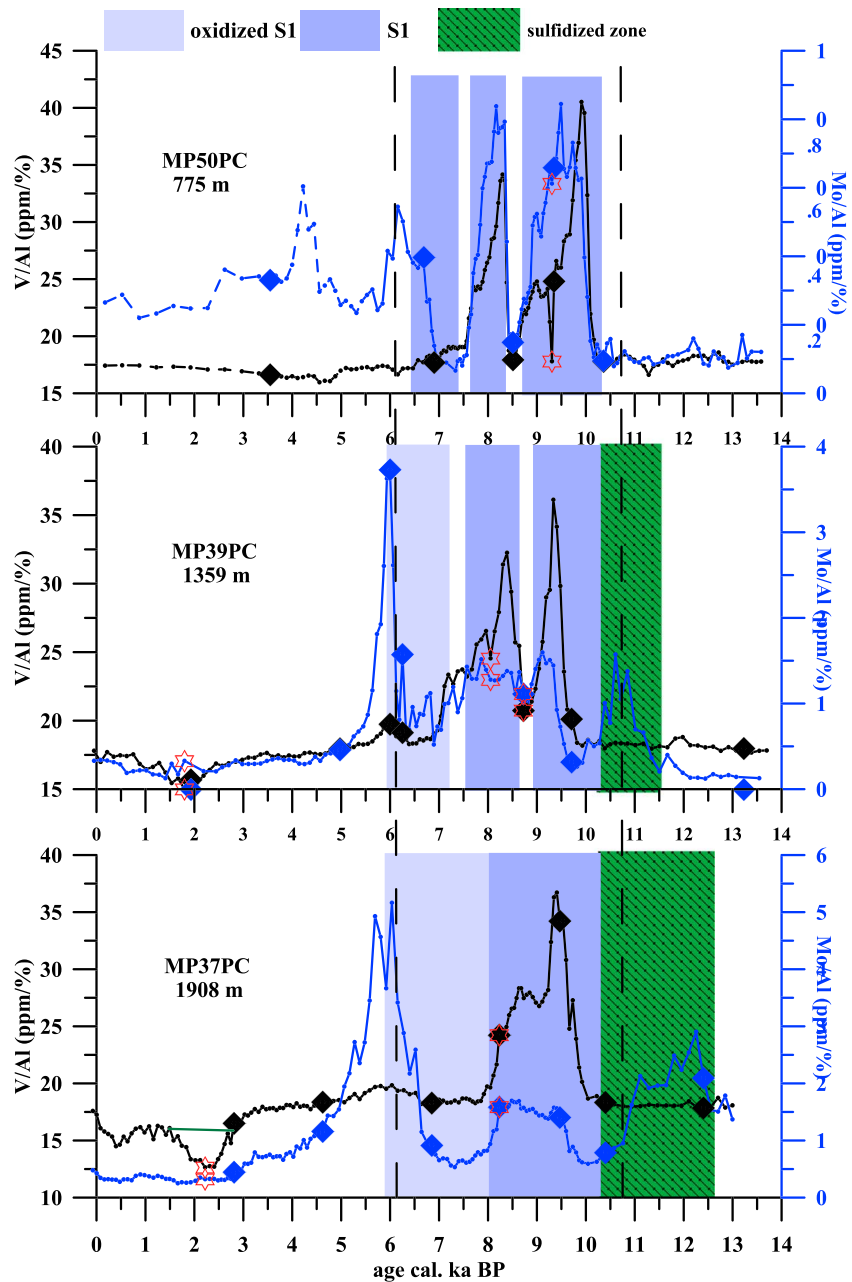


**Figure 7.** Fe (ox)/Al (%) (black line) and  $S_{\text{tot}}/\text{Al}$  (%; blue line). For dashed lines, symbols, and shading, see caption of Figure 4; for green shaded area, see caption of Figure 6.

preservation. Consequently, higher amounts of sulfides have been produced within the sapropel interval and exported downward during its formation, at the 1,908-m site than at the 1,359-m site. Such higher sulfide formation rates must be related to enhanced organic carbon content and more severe bottom-water anoxic conditions. This points to stronger anoxic and potentially higher sulfidic bottom waters at greater depths. Additionally, the absence of such sulfidization zone for the more shallow 775-m site, indicates that there was no excess sulfide formation in these sapropelic sediments. This is thought to relate to the diminished rate of sulfate reduction in the shallow core due to lower reactive organic matter content and the relatively large amount of Fe oxides due to a high sedimentation rate. This lower reactive organic matter content is related to a lower degree of preservation in the more shallow bottom waters that are thought not to have been permanently anoxic (De Lange et al., 2008; Filippidi et al., 2016; Reitz et al., 2006).

Consequently, during the lowermost S1 phase (S1a), the 1,908-m site was more anoxic than the 1,359-m site, whereas the most shallow 775-m site was rather moderately anoxic.

### 3.3.2. Oxidation Front

The second diagenetic process is taking place after the reventilation of the bottom water at the end of sapropel formation. The subsequent permanently oxic bottom-water conditions, lead to the penetration of oxygen into the sapropel layer and the consequent downward progressing oxidation of organic matter and pyrite (De Lange et al., 1989; Pruyssers et al., 1991; Reitz et al., 2006; Thomson et al., 1995, 1999; Van Santvoort et al., 1996). At the two deeper sites, the occurrence of a postdepositional oxidation front at the topmost part of the sapropel is prominent (Figure 4). In both cores, TOC(%) and S/Al profiles indicate that the upper part of the sapropel has been oxidized and hence organic matter and pyrite have been removed. However, the Ba/Al ratio remains unaffected and still represents the initial extent of the sapropel layer (Figures 4 and 5). At these two sites, the lower manganese and Fe (ox) peaks within the Ba-enriched interval demonstrate that the oxidation front has extended to 10 and 15 cm at MP39 and MP37 site; thus, the “residual” unoxidized sapropel (i.e., sapropel part preserving its geochemical signal) is still present in sediment older than 7 and 8 cal. ka BP respectively. For the most shallow site, MP50PC, such downward oxidation front is not apparent. The high sediment accumulation rate must have prevented the downward oxidation of sapropel sediments here (Mercone et al., 2000, 2001).

## 3.4. Organic-Rich Interval—Sapropel S1

### 3.4.1. Paleoproductivity and Organic Matter Preservation During S1

Significant enrichments in Ba/Al ratios in sapropels are thought to be related to enhanced primary production in the surface waters, resulting in enhanced water column formation and subsequent deposition and preservation of marine barite at the seafloor (Bishop, 1988; Dymond et al., 1992; Martinez-Ruiz et al., 2000; Thomson et al., 1995; Van Os et al., 1994). This excess Ba results from barite formation associated with decaying organic matter while settling in the water column (Bishop, 1988; Dymond et al., 1992; Klump et al., 2000; Möbius et al., 2010) and can be used to assess (qualitatively) the bottom-arriving organic fluxes (Eagle et al., 2003). Furthermore, it has been shown that due to moderate sulfate reduction in Holocene Mediterranean sediments, pore water sulfate depletion has not occurred during sapropel S1 formation. Therefore, barite has not been affected by diagenetic dissolution (Martinez-Ruiz et al., 2000; Nijenhuis et al., 1999; Passier et al., 1999; Thomson et al., 1995; van Santvoort et al., 1996). At the two deeper sites, MP39 (1,359 m) and MP37 (1,908 m), Ba/Al ratios as well as the organic matter concentrations reach notably higher values compared to the intermediate water depth 775-m site (Figure 5). A linear relation between organic matter contents and water depth has been previously reported and ascribed to reduced organic matter degradation (De Lange et al., 1989; Murat & Got, 2000). Similarly, excess Ba concentration has been noted to increase with water depth as a result of longer residence time of settling particulate organic matter in the water column and therefore more time available for the formation of barite (Dymond et al., 1992; von Breyman et al., 1992; Weldeab et al., 2003). Thus, the higher concentrations in Ba/Al and TOC(%) during S1 deposition delineate enhanced biological production in the surface waters, whereas decreased oxygen conditions at the seafloor facilitate the enhanced preservation of organic matter. Accordingly, the different concentrations between the deep and shallow sites reflect increasing preservation potential with water depth (De Lange et al., 2008).

### 3.4.2. Water Column and Depositional Setting During S1 for Different Water Depths

Pre-S1 and post S1, Mn/Al ratios are higher than during S1 in all cores, suggesting oxic conditions before and after sapropel deposition. The low Mn/Al values during S1 reflect the predominant absence of oxic conditions thus mobilization of Mn oxides. The low remaining Mn/Al merely represents the clay-, mineral-, and carbonate-associated Mn content.

Based on the more pronounced variability at the high sedimentation rate intermediate water depth 775-m site MP50PC, sapropel formation can be divided in three periods. The first period S1a is from the beginning of sapropel formation until the 8.2 cal. ka BP reventilation event (after Rohling, 1994). The second period extends from 8.2 to 7.4 cal. ka BP, and the third one from 7.4 cal ka BP until the end of sapropel conditions. The second and third part together are equivalent to the S1b period (sensu Rohling, 1994). We will refer to these as S1b-1 and S1b-2, respectively (Figures 4 and 5).

During the first period, that is, S1a (10.2–8.2 cal. ka BP), severely anoxic conditions prevailed for all three cores and water depths. Redox-sensitive elements' profiles exhibit a broad peak that concludes

temporarily at the ~8.2 cal. ka BP reventilation event. The V/Al profile is nearly identical to that of TOC(%). Higher levels of Mo, S, and Fe at the bottom of sapropel S1a interval corroborate the rapid development of anoxic and sulfidic conditions for bottom water and sediment/water interface (Figures 6 and 7). The ensued formation of iron-sulfides, mainly pyrite, during sapropel formation (Nijenhuis et al., 1999; Passier et al., 1996; 1999) and the presence of minor amounts of sulfide in the water column (Reed et al., 2011) act as a prerequisite for Mo scavenging from the water column (Algeo & Lyons, 2006; Algeo & Maynard, 2004; Algeo & Rowe, 2012; Helz et al., 1996; Tribouillard et al., 2006; Zheng et al., 2000). Thus, based on S/Al and Mo/Al ratios, this period is characterized by prolonged development of not only sulfidic sediments at the shallow site (MP50) but potentially also sulfidic bottom waters at the two deeper sites (MP39 and MP37; Azrieli-Tal et al., 2014; Reed et al., 2011; Scheiderich et al., 2010; Thomson et al., 1999; Warning & Brumsack, 2000). At the transitional water depth site (MP39), small fluctuations in the Mo/Al profile suggest that the interruption at 8.2 cal. ka affected the sediments and bottom water at this site, whereas the Mo/Al ratio at the deeper site (MP37PC) remains high throughout the whole residual sapropel layer, that is, until ~8 cal. ka BP. Hence, there is no detectable evidence that such an interruption has affected the deeper site.

During the second part of sapropel formation, that is, S1b-1 (~8.2 to 7.4 cal. ka BP), at the intermediate and transitional water depth sites MP50PC and MP39PC, sapropel formation resumed rapidly; thus, anoxic conditions at the sediment/water interface reinstated and deposition of high fluxes of organic matter continued as well as their preservation at the seafloor. Redox-sensitive elements' contents as well as Ba/Al and TOC(%) appear elevated during this interval at these two sites. At the deepest site, postdepositional oxidation of the sediments, younger than ~8 cal. ka BP, has altered the sediment geochemical composition; thus, the trace elemental and TOC%, S/Al profiles do not represent initial depositional conditions (see section 3.3.2).

The last part of the sapropel, that is, S1b-2 (7.4–6.5 cal. ka BP) has remained unaffected by postdepositional oxidation for the intermediate water depth 775-m site alone. Thus, here it still fully represents the initial depositional composition (see section 3.3.2). At the two deeper sites, the Ba/Al ratio indicates that enhanced primary production and barite-Ba formation and preservation persisted until the end of sapropel deposition but other proxies have been degraded by postdepositional oxidation. For the shallow 775-m site, the Ba/Al ratio and TOC(%) reduce gradually from 7.4 cal. ka BP onward suggesting the continuation of high organic carbon fluxes to the seafloor, but under intermittently oxic conditions. Redox-sensitive elements remain low and gradually reach background values.

Thus, during the last phase of sapropel formation, the depositional environment only gradually adjusted to less stagnant conditions for the transitional to deep water sites. In contrast, for the intermediate water 775-m site there must have been irregular ventilation events as environmental conditions remained suboxic to intermittently oxic after the 7.4-cal ka ventilation event.

### 3.5. Initiation of Sapropel (S1) Formation

It has been previously suggested that processes leading to sapropel formation, that is, humid climate conditions, water column stagnation and/or increased primary productivity, started earlier than the reported age based on sedimentary records (de Lange et al., 2008; Rohling et al., 1993; Tachikawa et al., 2015; van Helmond et al., 2015). Northward migration of ITCZ promoted moisture transfer above the basin as well as enhanced runoff, thus leading to the hampering of deepwater ventilation. (Bosmans et al., 2015; Emeis et al., 2000, 2003; Grant et al., 2012; Marino et al., 2009; Rohling et al., 2015; Tzedakis, 2007). Furthermore, deglaciation may have triggered the initial stratification of the water column thus facilitating the onset of sapropel formation (Cornuault et al., 2018; Grimm et al., 2015; Rohling et al., 2015). It seems likely that stagnation and thus conditions facilitating preservation initiated at greater depths, whereas biological activity in the surface waters must have been uniform in the study area.

Ba/Al and TOC(%) profiles in all three cores indicate that enhanced fluxes of organic carbon were exported from the surface waters and were deposited and preserved at the seafloor (Figure 5). The onset of sapropel formation for our three cores on a bathymetric transect appears to have been nearly synchronous for all water depths and to coincide with the basin-wide reported age for this event (De Lange et al., 2008). Similar ages ranging from ~10.0 to 10.8 have been previously suggested based on different proxies from different regions and water depths (e.g., Abu-Zied et al., 2008; Hennekam et al., 2014; Kuhnt et al., 2007; Mercone et al., 2001; Schmiedl et al., 2010; Triantaphyllou et al., 2009) all suggesting that anoxic

conditions were rapidly established in the basin. The observed potential difference in timing is small ( $\sim 0.8$  ka) and taking into account uncertainties imposed by radiocarbon dating ( $\pm 0.04$  ka), reservoir age ( $\pm 0.06$ ), sampling and processing ( $\sim 0.3$  ka), and calibration and construction of the age model ( $\pm 0.4$ ), a synchronous development of conditions favorable to sapropel preservation, that is, anoxic conditions, is confirmed. The Ba/Al, Mo/Al, and V/Al ratios and TOC(%) suggest that the transition to reducing conditions occurred rapidly (De Lange et al., 2008; Tesi et al., 2017).

### 3.6. Ending of Sapropel (S1) Formation

The final restoration of normal oxic water column conditions corresponds with the full resumption of DW-formation and thereby the basin-wide oxygenation of bottom waters (De Lange et al., 1989; De Lange et al., 2008; Reed et al., 2011; Reitz et al., 2006; van Santvoort et al., 1996). The sharp peak in each Mn/Al profile, that is, the Mn-MB, marks this onset of repetitive ventilation and associated continuous supply of oxygen to the deep water (Figure 4). At the shallower site, full reoxygenation of bottom waters seems to have occurred at  $\sim 6.6 \pm 0.3$  cal. ka BP, after a period of already intermittently oxic conditions. However, at 1,359- and 1,908-m water depth sites, it seems to have occurred at  $\sim 6.0 \pm 0.3$  cal. ka BP. The latter age is concordant with the basin-wide reventilation age for the Eastern Mediterranean (De Lange et al., 2008), which resulted in the formation of the Marker Bed. This event is expected to be synchronous in the entire basin; hence, the slight offset in timing—if true—can be explained by the successive, temporal downward progressing of oxygenated waters. An earlier ending or progressive oxygenation has been suggested based on benthic fauna in the Aegean and Adriatic Sea and on geochemical data in the Adriatic Sea (Jorissen et al., 1993; Rohling et al., 1997; Schmiedl et al., 2010; Tachikawa et al., 2015). In a recent paper, such progressive oxygenation or rather “more frequent oxygenation events” has been detailed for core MP50PC outlining that this may well explain reported differences in sapropel S1 ending based on different proxies (Filippidi et al., 2016). At shallow depths already before the end of sapropel formation, bottom waters have been more frequently oxic, whereas at greater water depths the higher frequency of reventilation occurred slightly later. The high-resolution sampling in addition to the key location of the studied cores at the embouchure of Adriatic DW-formation and the firm age models have allowed us to observe this potentially progressive recovery of the system. In the progressively decreasing humid conditions, that is, decreasing runoff, an initial period of sporadic Adriatic-sourced DW-formation could have preceded the full DW resumption. Similarly, present-day dense shelf-water formation in Adriatic Sea shows a density-related variability of cascading events that in turn controls the penetration depth of the newly formed water mass (Langone et al., 2016).

Furthermore, the great difference in Mn/Al ratios at the Marker Bed are notably higher at the two deeper sites (1,359 and 1,908 m), up to 3 times higher, outlining that dissolved  $\text{Mn}^{2+}$  remobilization continued until the final reventilation. At the shallow site, due to repetitive pulses of oxygenated waters, recycling of manganese oxides did not allow substantial growth of dissolved manganese in the bottom water nor its mobilization from the sediment.

### 3.7. Interruption and Reventilation of Bottom Water

At the intermediate water depth 775-m site, peaks can be observed in the Mn/Al ratio at  $\sim 8.2$  and 7.4 cal. ka BP, suggesting the resupply of oxygen to the bottom water and the subsequent precipitation of  $\text{MnO}_2$  in the sediments (Figure 4). The 8.2-cal. ka BP interruption of sapropel formation is expressed in our records of the shallow MP50PC site and to a lesser extent in those of the transitional site, MP39PC, whereas it cannot be detected in the deep site MP37PC. The detection of such brief episode depends on sample resolution, whereas its expression/preservation appears to be related to water depth. Higher sedimentation rate records have yielded the interruption of sapropel formation at 8.2 cal. ka BP basin wide, as well as the gradual oxygenation of the bottom waters that have been followed by a rapid reestablishment of reducing conditions after this cold episode (Almogi-Labin et al., 2009; Casford et al., 2001; Marino et al., 2009). In concert, Ba/Al ratio and TOC(%) show a more pronounced decline at 8.2 ka for the intermediate water depth 775-m site and a less prominent decrease for the transitional 1,359-m site, suggesting the temporary halt of enhanced preservation. Furthermore, the depiction of such a short event at these water depths points to a decrease in preservation potentially due to oxygen supply and ventilation to these water depths.

Similarly, the second reoxygenation event at 7.4 cal. ka BP is also recorded at these two sites indicating that once again a rapid cooling of surface waters triggered the restart of DW-formation to water depths at least as

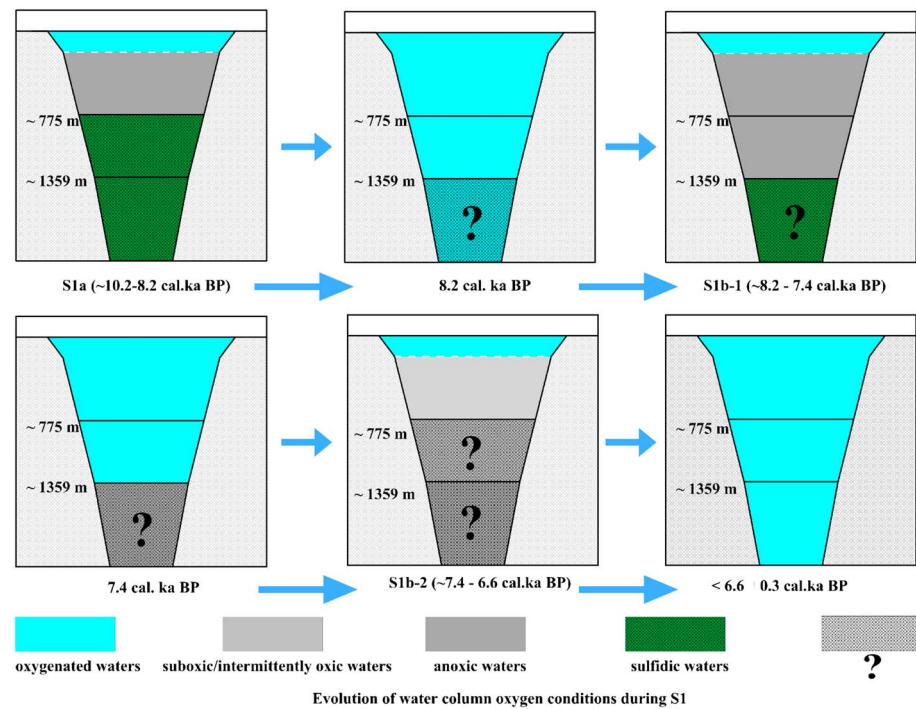


**Figure 8.** Schematic view of sequential water column oxygen conditions for different time slices. For intervals where information is not preserved in our records (noted with “?”), we base our results on information from reported bottom-water oxygen conditions in the literature. Pre-S1a conditions were oxidic for all water depths.

deep as MP39PC site (1,359 m). This cooling event is detectable at these sites, which are under the immediate influence of DW-formation, whereas it has been previously reported also for the Aegean Sea (e.g., Filippidi et al., 2016; Kouli et al., 2012; Triantaphyllou et al., 2016).

### 3.8. Implications for the Basin-Wide DW-Evolution

An integrated scenario can now be given for the sequentially developing DW-formation and related basin-wide water column conditions (Figure 8). Rapidly increasing, climate-induced enhanced runoff results in promptly developing bottom-water stagnation and the isochronous onset of sapropel S1 formation.

The first period of sapropel formation (10.6–8.2 cal. ka BP—S1a) is characterized by overall anoxic conditions at intermediate water levels and sulfidic sediments and possibly bottom waters in transitional and deepwater levels (S/Al, Mo/Al, and V/Al). Conditions are likely to have been more sulfidic for the deepest, 1,908-m site than for the transitional 1,359-m site.

A rapid episode of DW-formation and thus bottom-water reoxygenation is profoundly depicted in our intermediate and transitional water depth sites, at ~8.2 cal. ka BP. Hence, dense oxidic waters penetrated the water column down to approximately 1.4 km or even deeper. We cannot confidently evaluate this for the 1,908-m site as proxies have been eliminated due to postdepositional diagenetic oxidation of sedimentary components down to ~8 ka.

A second period of confinement of DW-formation followed this interruption event and lasted until ~7.4 cal. ka BP (i.e., S1b-1; see section 3.7). During this period, oxygen-free conditions reinstated at all water depths and anoxic/sulfidic sediment and possibly bottom-water conditions developed at all depths.

At 7.4 cal. ka BP, a second DW-ventilation event allowed the temporary recovery of bottom-water oxygen conditions down to 1.4 km.

After the 7.4-cal. ka BP interruption, anoxic/sulfidic conditions are thought to have recovered only for the transitional and deep water but not for the intermediate water depth, that is, 775-m site. Thus, during the last period of S1 formation (S1b-2) periodic ventilation of bottom waters recurred at intermediate water depths (as indicated by low but still slightly enhanced S/Al and V/Al; slightly enhanced Mn/Al; gradually

increasing Fe (ox)/Al). Taken all evidence together, it seems that for the intermediate water 775-m site, there is a progressive recovery of water circulation increasingly affecting the water masses until and possibly beyond this depth level. Thus, although organic fluxes (Ba/Al) may persist for all depth levels, their seafloor preservation is progressively decreased, in particular for the most shallow site of our study (775 m). The Mn-MB marks the final basin-wide termination of sapropel S1 formation. Such progressive reventilation observed in the intermediate water site is consistent with a slightly earlier ending of S1 (based on Mn-MB, Mo/Al, and Ba/Al) for intermediate (775 m) versus transitional/deep water (1,359/1,908 m). However, the derived values of  $\sim 6.6 \pm 0.3$  versus  $\sim 6.0 \pm 0.3$  cal. ka BP are within error and similar to the previously derived basin-wide ending of S1 ( $6.1 \pm 0.5$  cal. ka BP; De Lange et al., 2008).

#### 4. Conclusions

We studied in high resolution three high sedimentation rate cores in a bathymetric transect under the direct influence of DW-formation from the South Adriatic Sea, that is, from 779-m (MP50PC), 1,359-m (MP39PC), and 1,908-m (MP37PC) water depth.

1. The sedimentation rate during sapropel S1 was considerably enhanced for all three sites, providing the first direct proof for enhanced river runoff originating from northern borderlands concomitant to that from the southern borderlands, that is, during the North African humid period.
2. Sapropel deposition has occurred under variable redox conditions in the sediment and bottom waters for different water depths.
3. At the intermediate water depth site (775 m), during the first part of sapropel deposition, bottom-water conditions appear to have been severely anoxic, whereas during the last part, that is,  $>7.4$  cal. ka BP onward, these have been intermittently oxic. In contrast, at the two deeper sites (1,359 and 1,908 m), sediment and bottom-water conditions have been persistently anoxic and sulfidic leading to excess sulfide formation and the development of a sulfidization zone beneath the sapropel. The absence of such a zone at the shallower site indicates that bottom waters during S1 deposition have not been sulfidic at intermediate water depth.
4. Distinct reventilation events occurred at 8.2 and 7.4 cal. ka BP, leading to brief oxidation pulses down to  $\sim 1.4$  km.
5. The full resumption of DW-formation must have been synchronous in the entire basin but the full re-oxygenation of the bottom water at intermediate water depth is thought to have been more gradual. The end of oxygen-restricted conditions, as indicated by Mn/Al, has occurred progressively for the 775-m site where fully oxic conditions have been restored at  $\sim 6.6 \pm 0.3$  cal. ka BP. Although within error, full oxygenation for the deeper sites is thought to have occurred slightly later, namely, at  $\sim 6.0 \pm 0.3$  cal. ka BP.

#### Acknowledgments

We are grateful to captain, crew, and scientific team on board RV *Pelagia* for cores' collection and Dineke van de Meent-Olieman, Helen de Waard, Ton Zalm, and Arnold van Dijk for analytical assistance. The Dutch Science Foundation (NWO. 817.01.002 Moccha) and the European Science Foundation (ESF) Eurocores Programme EuroMARC are acknowledged for their financial support of the MOCCHA- project and MACCHIATO-cruise. We thank Donatella Insinga for tephra analyses, Rick Hennekam for assisting in constructing the age models, Antonio Schirone for  $^{210}\text{Pb}$  preliminary results, and Vasilis Anagnostopoulos for assisting in creating Figure 1. We thank one anonymous reviewer, Leonardo Langone and Editor Stephen Barker for their constructive comments that were helpful to revise and improve our paper. Data used are uploaded in Pangaea data repository (Filippidi & De Lange, 2018): doi:10.1594/PANGAEA.896932. We confirm that there are no known conflicts of interest, financial or otherwise, associated with this publication for any of the listed authors.

#### References

- Abu-Zied, R. H., Rohling, E. J., Jorissen, F. J., Fontanier, C., Casford, J. S. L., & Cooke, S. (2008). Benthic foraminiferal response to changes in bottom-water oxygenation and organic carbon flux in the eastern Mediterranean during LGM to Recent times. *Marine Micropaleontology*, 67(1–2), 46–68. <http://doi.org/10.1016/j.marmicro.2007.08.006>
- Algeo, T. J., & Lyons, T. W. (2006). Mo-total organic carbon covariation in modern anoxic marine environments: Implications for analysis of paleoredox and paleohydrographic conditions. *Paleoceanography*, 21, PA1016. <https://doi.org/10.1029/2004PA001112>
- Algeo, T. J., & Maynard, J. B. (2004). Trace-element behavior and redox facies in core shales of Upper Pennsylvanian Kansas-type cyclothems. *Chemical Geology*, 206(3–4), 289–318. <http://doi.org/10.1016/j.chemgeo.2003.12.009>
- Algeo, T. J., & Rowe, H. (2012). Paleoceanographic applications of trace-metal concentration data. *Chemical Geology*, 324–325, 6–18. <http://doi.org/10.1016/j.chemgeo.2011.09.002>
- Alley, R. B., Mayewski, P. A., Sowers, T., Stuiver, M., Taylor, K. C., & Clark, P. U. (1997). Holocene climatic instability: A prominent, widespread event 8200 yr ago. *Geology*, 25(6), 483–486. [http://doi.org/10.1130/0091-7613\(1997\)025<0483](http://doi.org/10.1130/0091-7613(1997)025<0483)
- Almogi-Labin, A., Bar-Matthews, M., Shriki, D., Kolosovsky, E., Paterne, M., Schilman, B., et al. (2009). Climatic variability during the last  $\sim 90$ ka of the southern and northern Levantine Basin as evident from marine records and speleothems. *Quaternary Science Reviews*, 28(25–26), 2882–2896. <http://doi.org/10.1016/j.quascirev.2009.07.017>
- Ariztegui, D., Asioli, A., Lowe, J. J., Trincardi, F., Vigliotti, L., Tamburini, F., et al. (2000). Palaeoclimate and the formation of sapropel S1: Inferences from late quaternary lacustrine and marine sequences in the Central Mediterranean region. *Palaeogeography, Palaeoclimatology, Palaeoecology*, 158(3–4), 215–240. [http://doi.org/10.1016/S0031-0182\(00\)00051-1](http://doi.org/10.1016/S0031-0182(00)00051-1)
- Arnaboldi, M., & Meyers, P. A. (2007). Trace element indicators of increased primary production and decreased water-column ventilation during deposition of latest Pliocene sapropels at five locations across the Mediterranean Sea. *Palaeogeography, Palaeoclimatology, Palaeoecology*, 249(3–4), 425–443. <http://doi.org/10.1016/j.palaeo.2007.02.016>
- Azrieli-Tal, I., Matthews, A., Bar-Matthews, M., Almogi-Labin, A., Vance, D., Archer, C., & Teutsch, N. (2014). Evidence from molybdenum and iron isotopes and molybdenum-uranium covariation for sulphidic bottom waters during Eastern Mediterranean sapropel S1 formation. *Earth and Planetary Science Letters*, 393, 231–242. <http://doi.org/10.1016/j.epsl.2014.02.054>

- Bar-Matthews, M., Ayalon, A., Kaufman, A., & Wasserburg, G. J. (1999). The Eastern Mediterranean paleoclimate as a reflection of regional events: Soreq cave, Israel. *Earth and Planetary Science Letters*, *166*(1–2), 85–95. [http://doi.org/10.1016/S0012-821X\(98\)00275-1](http://doi.org/10.1016/S0012-821X(98)00275-1)
- Bishop, J. K. B. (1988). The barite-opal-organic carbon association in oceanic particulate matter. *Nature*, *332*, 341–343. <https://doi.org/10.1038/332341a0>
- Blaauw, M., & Christen, J. A. (2005). Radiocarbon peat chronologies and environmental change. *Journal of the Royal Statistical Society. Series C: Applied Statistics*, *54*(4), 805–816. <http://doi.org/10.1111/j.1467-9876.2005.00516.x>
- Blaauw, M., & Christen, J. A. (2011). Flexible paleoclimate age-depth models using an autoregressive gamma process. *Bayesian Analysis*, *6*(3), 457–474. <http://doi.org/10.1214/11-BA618>
- Bosmans, J. H. C., Drijfhout, S. S., Tuenter, E., Hilgen, F. J., Lourens, L. J., & Rohling, E. J. (2015). Precession and obliquity forcing of the freshwater budget over the Mediterranean. *Quaternary Science Reviews*, *123*, 16–30. <http://doi.org/10.1016/j.quascirev.2015.06.008>
- Bout-Roumazeilles, V., Combourieu-Nebout, N., Desprat, S., Siani, G., Turon, J.-L., & Essallami, L. (2013). Tracking atmospheric and riverine terrigenous supplies variability during the last glacial and the Holocene in central Mediterranean. *Climate of the Past*, *9*(3), 1065–1087. <http://doi.org/10.5194/cp-9-1065-2013>
- Brumsack, H.-J. (1989). Geochemistry of recent TOC-rich sediments from the Gulf of California and the Black Sea. *Geologische Rundschau*, *78*(3), 851–882. <http://doi.org/10.1007/BF01829327>
- Calvert, S. E. (1983). Geochemistry of Pleistocene sapropels and associated sediments from the Eastern Mediterranean. *Oceanologica Acta*, *6*(3), 255–267.
- Calvert, S. E., & Fontugne, M. R. (1987). Stable carbon isotopic evidence for the marine origin of the organic matter in the Holocene black sea sapropel. *Chemical Geology: Isotope Geoscience Section*, *66*(3–4), 315–322. [http://doi.org/10.1016/0168-9622\(87\)90051-0](http://doi.org/10.1016/0168-9622(87)90051-0)
- Calvert, S. E., & Pedersen, T. F. (1993). Geochemistry of Recent oxic and anoxic marine sediments: Implications for the geological record. *Marine Geology*, *113*(1–2), 67–88. [http://doi.org/10.1016/0025-3227\(93\)90150-T](http://doi.org/10.1016/0025-3227(93)90150-T)
- Canals, M., Danovaro, R., Heussner, S., Lykousis, V., Puig, P., Trincardi, F., et al. (2009). Cascades in Mediterranean submarine grand canyons. *Oceanography*, *22*(1), 26–43. <http://doi.org/10.5670/oceanog.2009.03>
- Cantoni, C., Luchetta, A., Chiggiato, J., Cozzi, S., Schroeder, K., & Langone, L. (2016). Dense water flow and carbonate system in the southern Adriatic: A focus on the 2012 event. *Marine Geology*, *375*, 15–27. <http://doi.org/10.1016/j.margeo.2015.08.013>
- Casford, J. S. L., Abu-Zied, R., Rohling, E. J., Cooke, S., Boessenkool, K. P., Brinkhuis, H., et al. (2001). Mediterranean climate variability during the Holocene. *Mediterranean Marine Science*, *2*(1), 45–55. <https://doi.org/10.12681/mms.275>
- Casford, J. S. L., Rohling, E. J., Abu-Zied, R. H., Fontanier, C., Jorissen, F. J., Leng, M. J., et al. (2003). A dynamic concept for eastern Mediterranean circulation and oxygenation during sapropel formation. *Palaeogeography, Palaeoclimatology, Palaeoecology*, *190*, 103–119. [https://doi.org/10.1016/S0031-0182\(02\)00601-6](https://doi.org/10.1016/S0031-0182(02)00601-6)
- Castradori, D. (1993). Calcareous nannofossils and the origin of eastern Mediterranean sapropel. *Paleoceanography*, *8*(4), 459–471. <https://doi.org/10.1029/93PA00756>
- Christen, A. J., & Perez, S. E. (2009). A new robust statistical model for radiocarbon data. *Radiocarbon*, *51*(03), 1047–1059. <https://doi.org/10.1017/S003382220003410X>
- Cita, M. B., Camerlenghi, A., Erba, E., McCoy, F. W., Castradori, D., Cazzani, A., et al. (1989). Discovery of mud diapirism in the Mediterranean Ridge. A preliminary report. *Bollettino della Società geologica italiana*, *108*, 537–543.
- Combourieu-Nebout, N., Peyron, O., Bout-Roumazeilles, V., Goring, S., Dormoy, I., Joannin, S., et al. (2013). Holocene vegetation and climate changes in the central Mediterranean inferred from a high-resolution marine pollen record (Adriatic Sea). *Climate of the Past*, *9*(5), 2023–2042. <http://doi.org/10.5194/cp-9-2023-2013>
- Cornuault, M., Tachikawa, K., Vidal, L., Guihou, A., Siani, G., Deschamps, P., et al. (2018). Circulation changes in the Eastern Mediterranean Sea over the past 23,000 years inferred from Authigenic Nd isotopic ratios. *Paleoceanography and Paleoclimatology*, *33*, 264–280. <https://doi.org/10.1002/2017PA003227>
- Crusius, J., Calvert, S., Pedersen, T., & Sage, D. (1996). Rhenium and molybdenum enrichments in sediments as indicators of oxic, suboxic and sulfidic conditions of deposition. *Earth and Planetary Science Letters*, *145*(1–4), 65–78. [https://doi.org/10.1016/S0012-821X\(96\)00204-X](https://doi.org/10.1016/S0012-821X(96)00204-X)
- De Lange, G. J. (1986). Early diagenetic reactions in interbedded pelagic and turbiditic sediments in the Nares Abyssal Plain (western North Atlantic): Consequences for the composition of sediment and interstitial water. *Geochimica et Cosmochimica Acta*, *50*(12), 2543–2561. [http://doi.org/10.1016/0016-7037\(86\)90209-7](http://doi.org/10.1016/0016-7037(86)90209-7)
- De Lange, G. J., Jarvis, I., & Kuijpers, A. (1987). Geochemical characteristics and provenance of late Quaternary sediments from the Madeira Abyssal Plain, N Atlantic. *Geological Society Special Publication*, *31*(1), 147–165. <https://doi.org/10.1144/GSL.SP.1987.031.01.12>
- De Lange, G. J., & Ten Haven, H. L. (1983). Recent sapropel formation in the eastern Mediterranean. *Nature*, *305*, 797–798.
- De Lange, G. J., Van Os, B., Pruyssers, P. A., Middelburg, J. J., Castradori, D., Van Santvoort, P., et al. (1994). Possible early diagenetic alteration of palaeo proxies. In Zalm, et al. (Eds.), *NATO ASI Series* (Vol. 117, pp. 226–258). Berlin Heidelberg: Springer-Verlag. <http://doi.org/10.1086/421294>
- De Menocal, P., Ortiz, J., Guilderson, T., Adkins, J., Sarnthein, M., Baker, L., & Yarusinsky, M. (2000). Abrupt onset and termination of the African humid period: Rapid climate responses to gradual insolation forcing. *Quaternary Science Reviews*, *19*, 347–361.
- De Rijk, S., Hayes, A., & Rohling, E. J. (1999). Eastern Mediterranean sapropel S1 interruption: An expression of the onset of climatic deterioration around 7 ka BP. *Marine Geology*, *153*, 337–343.
- Dymond, J., Suess, E., & Lyle, M. (1992). Barium in deep-sea sediment: A geochemical proxy for paleoproductivity. *Paleoceanography*, *7*(2), 163–181. <https://doi.org/10.1029/92PA00181>
- Eagle, M., Paytan, A., Arrigo, K. R., van Dijken, G., & Murray, R. W. (2003). A comparison between excess barium and barite as indicators of carbon export. *Paleoceanography*, *18*(1), 1021. <https://doi.org/10.1029/2003PA000922>
- Emeis, K., Struck, U., Schulz, H., Rosenberg, R., Bernasconi, S., Erlenkeuser, H., et al. (2000). Temperature and salinity variations of Mediterranean Sea surface waters over the last 16,000 years from records of planktonic stable oxygen isotopes and alkenone unsaturation ratios. *Palaeogeography, Palaeoclimatology, Palaeoecology*, *158*, 259–280.
- Emeis, K.-C., Schulz, H., Struck, U., Rossignol-Strick, M., Erlenkeuser, H., Howell, M. W., et al. (2003). Eastern Mediterranean surface water temperatures and  $\delta^{18}\text{O}$  composition during deposition of sapropels in the late quaternary. *Paleoceanography*, *18*(1), L24708. <https://doi.org/10.1029/2000PA000617>
- Emerson, S. R., & Huested, S. S. (1991). Ocean anoxia and the concentrations of molybdenum and vanadium in seawater. *Marine Chemistry*, *34*(3–4), 177–196. [http://doi.org/10.1016/0304-4203\(91\)90002-E](http://doi.org/10.1016/0304-4203(91)90002-E)
- Filippidi, A., & De Lange, G. J. (2018). Geochemistry and  $\delta^{18}\text{O}$  G.ruber records of sediment cores MP50PC, MP39PC and MP37PC. *PANGAEA*. <https://doi.org/10.1594/PANGAEA.896932>

- Filippidi, A., Triantaphyllou, M. V., & De Lange, G. J. (2016). Eastern-Mediterranean ventilation variability during sapropel S1 formation, evaluated at two sites influenced by deep-water formation from Adriatic and Aegean seas. *Quaternary Science Reviews*, *144*, 95–106. <http://doi.org/10.1016/j.quascirev.2016.05.024>
- Froelich, P. N., Klinkhammer, G. P., Bender, M. L., Luedtke, N. A., Heath, G. R., Cullen, D., et al. (1979). Early oxidation of organic matter in pelagic sediments of the eastern equatorial Atlantic: Suboxic diagenesis. *Geochimica et Cosmochimica Acta*, *43*, 1075–1090. [http://doi.org/10.1016/0016-7037\(79\)90095-4](http://doi.org/10.1016/0016-7037(79)90095-4)
- Gallego-Torres, D., Martínez-Ruiz, F., De Lange, G. J., Jiménez-Espejo, F. J., & Ortega-Huertas, M. (2010). Trace-elemental derived paleoceanographic and paleoclimatic conditions for Pleistocene eastern Mediterranean sapropels. *Palaeoecology, Palaeclimatology, Palaecology*, *293*(1–2), 76–89. <http://doi.org/10.1016/j.palaeo.2010.05.001>
- Goudeau, M. L. S., Grauel, A. L., Bernasconi, S. M., & de Lange, G. J. (2013). Provenance of surface sediments along the southeastern Adriatic coast off Italy: An overview. *Estuarine, Coastal and Shelf Science*, *134*, 45–56. <http://doi.org/10.1016/j.ecss.2013.09.009>
- Goudeau, M.-L. S., Grauel, A.-L., Tessarolo, C., Leider, A., Chen, L., Bernasconi, S. M., et al. (2014). The Glacial–Interglacial transition and Holocene environmental changes in sediments from the Gulf of Taranto, central Mediterranean. *Marine Geology*, *348*, 88–102. <http://doi.org/10.1016/j.margeo.2013.12.003>
- Grant, K. M., Grimm, R., Mikolajewicz, U., Marino, G., Ziegler, M., & Rohling, E. J. (2016). The timing of Mediterranean sapropel deposition relative to insolation, sea-level and African monsoon changes. *Quaternary Science Reviews*, *140*, 125–141. <http://doi.org/10.1016/j.quascirev.2016.03.026>
- Grant, K. M., Rohling, E. J., Bar-Matthews, M., Ayalon, A., Medina-Elizalde, M., Ramsey, C. B., et al. (2012). Rapid coupling between ice volume and polar temperature over the past 150,000 years. *Nature*, *491*(7426), 744–747. <http://doi.org/10.1038/nature11593>
- Grimm, R., Maier-Reimer, E., Mikolajewicz, U., Schmiedl, G., Müller-Navarra, K., Adloff, F., et al. (2015). Late glacial initiation of Holocene eastern Mediterranean sapropel formation. *Nature Communications*, *6*(1), 12pp. <http://doi.org/10.1038/ncomms8099>
- Helz, G. R., Miller, C. V., Charnock, J. M., Mosselmanns, J. F. W., Patrick, R. A. D., Garner, C. D., & Vaughan, D. J. (1996). Mechanism of molybdenum removal from the sea and its concentration in black shales: EXAFS evidence. *Geochimica et Cosmochimica Acta*, *60*(19), 3631–3642.
- Hennekam, R., Jilbert, T., Schnetger, B., & De Lange, G. J. (2014). Solar forcing of Nile discharge and sapropel S1 formation in the early to middle Holocene eastern Mediterranean. *Paleoceanography*, *29*, 1–14. <https://doi.org/10.1002/2013PA002553>
- Hilgen, F. J. (1991). Extension of the astronomically calibrated (polarity) time scale to the Miocene/Pliocene boundary. *Earth and Planetary Science Letters*, *107*(2), 349–368. [http://doi.org/10.1016/0012-821X\(91\)90082-S](http://doi.org/10.1016/0012-821X(91)90082-S)
- Jilbert, T., Reichert, G.-J., Mason, P., & De Lange, G. J. (2010). Short-time-scale variability in ventilation and export productivity during the formation of Mediterranean sapropel S1. *Paleoceanography*, *25*, PA4232. <https://doi.org/10.1029/2010PA001955>
- Jorissen, F. J., Asioli, A., Borsetti, A. M., Capotondi, L., Visse, J. P., De Hilgen, F. J., & Rohling, E. J. (1993). Late Quaternary central Mediterranean biochronology. *Marine Micropaleontology*, *21*, 169–189.
- Kallel, N., Paterne, M., Duplessy, J.-C., Vergnaud-Grazzini, C., Pujol, C., Labeyrie, L., et al. (1996). Enhanced rainfall in the mediterranean region during the last sapropel event. *Oceanologica Acta*, *20*(5), 697–712.
- Klump, J., Hebbeln, D., & Wefer, G. (2000). The impact of sediment provenance on barium-based productivity estimates. *Marine Geology*, *169*(3–4), 259–271. [http://doi.org/10.1016/S0025-3227\(00\)00092-X](http://doi.org/10.1016/S0025-3227(00)00092-X)
- Kotthoff, U., Pross, J., Müller, U. C., Peyron, O., Schmiedl, G., Schulz, H., & Bordon, A. (2008). Climate dynamics in the borderlands of the Aegean Sea during formation of sapropel S1 deduced from a marine pollen record. *Quaternary Science Reviews*, *27*(7–8), 832–845. <http://doi.org/10.1016/j.quascirev.2007.12.001>
- Kouli, K., Gogou, A., Bouloubassi, I., Triantaphyllou, M. V., Ioakim, C., Katsouras, G., et al. (2012). Late postglacial paleoenvironmental change in the northeastern Mediterranean region: Combined palynological and molecular biomarker evidence. *Quaternary International*, *261*, 118–127. <http://doi.org/10.1016/j.quaint.2011.10.036>
- Kuhnt, T., Schmiedl, G., Ehrmann, W., Hamann, Y., & Hemleben, C. (2007). Deep-sea ecosystem variability of the Aegean Sea during the past 22 kyr as revealed by benthic foraminifera. *Marine Micropaleontology*, *64*(3–4), 141–162. <http://doi.org/10.1016/j.marmicro.2007.04.003>
- Lange, G. J., Middelburg, J. J., & Pruyssers, P. A. (1989). Middle and Late Quaternary depositional sequences and cycles in the eastern Mediterranean. *Sedimentology*, *36*(1), 151–156. <https://doi.org/10.1111/j.1365-3091.1989.tb00827.x>
- de Lange, G. J., Thomson, J., Reitz, A., Slomp, C. P., Principato, M. S., Erba, E., & Corselli, C. (2008). Synchronous basin-wide formation and redox-controlled preservation of a Mediterranean sapropel. *Nature Geoscience*, *1*(9), 606–610. <http://doi.org/10.1038/ngeo283>
- Langone, L., Conese, I., Miserochi, S., Boldrin, A., Bonaldo, D., Carniel, S., et al. (2016). Dynamics of particles along the western margin of the Southern Adriatic: Processes involved in transferring particulate matter to the deep basin. *Marine Geology*, *375*, 28–43. <http://doi.org/10.1016/j.margeo.2015.09.004>
- Lascaratos, A. (1993). Estimation of deep and intermediate water mass formation rates in the Mediterranean Sea. *Deep Sea Research Part II: Topical Studies in Oceanography*, *40*(6), 1327–1332. [https://doi.org/10.1016/0967-0645\(93\)90072-U](https://doi.org/10.1016/0967-0645(93)90072-U)
- Lourens, L. J. (2004). Revised tuning of Ocean Drilling Program site 964 and KC01B (Mediterranean) and implications for the  $\delta^{18}\text{O}$ , tephra, calcareous nannofossil, and geomagnetic reversal chronologies of the past 1.1 Myr. *Paleoceanography*, *19*, PA3010. <https://doi.org/10.1029/2003PA000997>
- Magny, M., Combourieu-Nebout, N., de Beaulieu, J. L., Bout-Roumazeilles, V., Colombaroli, D., Desprat, S., et al. (2013). North–south palaeohydrological contrasts in the Central Mediterranean during the Holocene: Tentative synthesis and working hypotheses. *Climate of the Past*, *9*(5), 2043–2071. <http://doi.org/10.5194/cp-9-2043-2013>
- Malanotte-Rizzoli, P., Manca, B. B., d'Alcala, M. R., Theocharis, A., Bergamasco, A., Bregant, D., et al. (1997). A synthesis of the Ionian Sea hydrography, circulation and water mass pathways during POEM-Phase I. *Progress in Oceanography*, *39*, 153–204. [https://doi.org/10.1016/S0079-6611\(97\)00013-X](https://doi.org/10.1016/S0079-6611(97)00013-X)
- Malanotte-Rizzoli, P., Manca, B. B., d'Alcala, M. R., Theocharis, A., Brenner, S., Budillon, G., & Ozsoy, E. (1999). The eastern Mediterranean in the 80s and in the 90s: The big transition in the intermediate and deep circulations. *Dynamics of Atmospheres and Oceans*, *29*(2–4), 365–395. [http://doi.org/10.1016/S0377-0265\(99\)00011-1](http://doi.org/10.1016/S0377-0265(99)00011-1)
- Mangini, A., Eisenhauer, A., & Walter, P. (1990). Response of manganese in the ocean to the climatic cycles in the Quaternary. *Paleoceanography*, *5*(5), 811–821. <https://doi.org/10.1029/PA005i005p00811>
- Marino, G., Rohling, E. J., Sangiorgi, F., Hayes, A., Casford, J. L., Lotter, A. F., et al. (2009). Early and middle Holocene in the Aegean Sea: Interplay between high and low latitude climate variability. *Quaternary Science Reviews*, *28*(27–28), 3246–3262. <http://doi.org/10.1016/j.quascirev.2009.08.011>

- Martinez-Ruiz, F., Kastner, M., Paytan, A., Ortega-Huertas, M., & Bernasconi, S. M. (2000). Geochemical evidence for enhanced productivity during S1 sapropel deposition in the eastern Mediterranean. *Paleoceanography*, *15*(2), 200–209. <https://doi.org/10.1029/1999PA000419>
- Mercone, D., Thomson, J., Abu-Zied, R. H., Croudace, I. W., & Rohling, E. J. (2001). High-resolution geochemical and micropaleontological profiling of the most recent eastern Mediterranean sapropel. *Marine Geology*, *177*(1–2), 25–44. [https://doi.org/10.1016/S0025-3227\(01\)00122-0](https://doi.org/10.1016/S0025-3227(01)00122-0)
- Mercone, D., Thomson, J., Croudace, W., Siani, G., Paterne, M., & Troelstra, S. (2000). Duration of S1, the most recent sapropel in the eastern Mediterranean Sea, as indicated by accelerator mass spectrometry radiocarbon and geochemical evidence. *Paleoceanography*, *15*(3), 336–347. <https://doi.org/10.1029/1999PA000397>
- Meyer, K. M., & Kump, L. R. (2008). Oceanic Euxinia in earth history: Causes and consequences. *Annual Review of Earth and Planetary Sciences*, *36*(1), 251–288. <http://doi.org/10.1146/annurev.earth.36.031207.124256>
- Möbius, J., Lahajnar, N., & Emeis, K.-C. (2010). Diagenetic control of nitrogen isotope ratios in Holocene sapropels and recent sediments from the Eastern Mediterranean Sea. *Biogeosciences*, *7*(11), 3901–3914. <http://doi.org/10.5194/bg-7-3901-2010>
- Moodley, L., Middelburg, J. J., Herman, P. M. J., Soetaert, K., & de Lange, G. J. (2005). Oxygenation and organic-matter preservation in marine sediments: Direct experimental evidence from ancient organic carbon-rich deposits. *Geology*, *33*(11), 889–892. <http://doi.org/10.1130/G21731.1>
- Murat, A., & Got, H. (2000). Organic carbon variations of the eastern Mediterranean Holocene sapropel: A key for understanding formation processes. *Palaeogeography, Palaeoclimatology, Palaeoecology*, *158*(3–4), 241–257. [http://doi.org/10.1016/S0031-0182\(00\)00052-3](http://doi.org/10.1016/S0031-0182(00)00052-3)
- Myers, P. G., Haines, K., & Rohling, E. J. (1998). Modeling the paleocirculation of the Mediterranean: The last glacial maximum and the Holocene with emphasis on the formation of sapropel S1. *Paleoceanography*, *13*(6), 586–606. <https://doi.org/10.1029/98PA02736>
- Nijenhuis, I. A., Bosch, H., Sinninghe Damste, J. S., Brumsack, H.-J., & De Lange, G. J. (1999). Organic matter and trace element rich sapropels and black shales: A geochemical comparison. *Earth and Planetary Science Letters*, *169*, 277–290. [https://doi.org/10.1016/S0012-821X\(99\)00083-7](https://doi.org/10.1016/S0012-821X(99)00083-7)
- Olauson, E. (1961). Studies of deep-sea cores. *Reports of the Swedish Deep-Sea Expedition, 1947-1948*, *8*, 337–391.
- Ozsoy, E., Unluata, U., Oğuz, T., Latif, M. A., Hecht, A., & Brenner, et al. (1991). A review of the Levantin Basin circulation and its variabilities during 1985–1988. *Dynamics of Atmospheres and Oceans*, *15*(3–5), 421–456. [https://doi.org/10.1016/0377-0265\(91\)90027-D](https://doi.org/10.1016/0377-0265(91)90027-D)
- Passier, H. F., Böttcher, M. E., & De Lange, G. J. (1999). Sulphur enrichment in organic matter of eastern Mediterranean Sapropels: A study of Sulphur isotope partitioning. *Aquatic Geochemistry*, *5*(1), 99–118. <https://doi.org/10.1023/A:1009676107330>
- Passier, H. F., & De Lange, G. J. (1998). Sedimentary sulfur and Iron chemistry in relation to the formation of Eastern Mediterranean Sapropels 1. In A. H. F. Robertson, K.-C. Emeis, C. Richter, & A. Camerlenghi (Eds.), *Proceedings of the Ocean Drilling Program, Scientific Results* (Vol. 160, pp. 249–259).
- Passier, H. F., Middelburg, J. J., De Lange, G. J., & Böttcher, M. E. (1997). Pyrite contents, microtextures, and sulfur isotopes in relation to formation of the youngest eastern Mediterranean sapropel. *Geology*, *25*(6), 519–522. [https://doi.org/10.1130/0091-7613\(1997\)025<0519:PCMASI>2.3.CO;2](https://doi.org/10.1130/0091-7613(1997)025<0519:PCMASI>2.3.CO;2)
- Passier, H. F., Middelburg, J. J., van Os, B. J. H., & De Lange, G. J. (1996). Diagenetic pyritisation under eastern Mediterranean sapropels caused by downward sulphide diffusion. *Geochimica et Cosmochimica Acta*, *60*(5), 751–763. [https://doi.org/10.1016/0016-7037\(95\)00419-X](https://doi.org/10.1016/0016-7037(95)00419-X)
- Pinardi, N., & Masetti, E. (2000). Variability of the large scale general circulation of the Mediterranean Sea from observations and modelling: A review. *Palaeogeography, Palaeoclimatology, Palaeoecology*, *158*(3–4), 153–173. [http://doi.org/10.1016/S0031-0182\(00\)00048-1](http://doi.org/10.1016/S0031-0182(00)00048-1)
- Poulos, S. E., Drakopoulos, P. G., & Collins, M. B. (1997). Seasonal variability in sea surface oceanographic conditions in the Aegean Sea (Eastern Mediterranean): An overview. *Journal of Marine Systems*, *13*, 225–244. [http://doi.org/10.1016/S0924-7963\(96\)00113-3](http://doi.org/10.1016/S0924-7963(96)00113-3)
- Prahl, F. G., Muehlhausen, L. A., & Lyle, M. (1989). An organic geochemical assessment of oceanographic conditions at Manop Site C over the past 26,000 years. *Paleoceanography*, *4*(5), 495–510. <https://doi.org/10.1029/PA004i005p00495>
- Pross, J., Kotthoff, U., Müller, U. C., Peyron, O., Dormoy, I., Schmiel, G., et al. (2009). Massive perturbation in terrestrial ecosystems of the eastern Mediterranean region associated with the 8.2 kyr B.P. Climatic event. *Geology*, *37*(10), 887–890. <http://doi.org/10.1130/G25739A.1>
- Pruyvers, P. A., De Lange, G. J., & Middelburg, J. J. (1991). Geochemistry of eastern Mediterranean sediments: Primary sediment composition and diagenetic alterations. *Marine Geology*, *100*, 137–154.
- Pruyvers, P. A., De Lange, G. J., Middelburg, J. J., & Hydes, D. J. (1993). The diagenetic formation of metal-rich layers in sapropel-containing sediments in the eastern Mediterranean. *Geochimica et Cosmochimica Acta*, *57*(3), 527–536. [http://doi.org/10.1016/0016-7037\(93\)90365-4](http://doi.org/10.1016/0016-7037(93)90365-4)
- Ramsey, C. B. (2008). Deposition models for chronological records. *Quaternary Science Reviews*, *27*(1–2), 42–60. <http://doi.org/10.1016/j.quascirev.2007.01.019>
- Reed, D. C., Slomp, C. P., & De Lange, G. J. (2011). A quantitative reconstruction of organic matter and nutrient diagenesis in Mediterranean Sea sediments over the Holocene. *Geochimica et Cosmochimica Acta*, *75*(19), 5540–5558. <http://doi.org/10.1016/j.gca.2011.07.002>
- Reimer, P. J., & McCormac, F. G. (2002). Marine radiocarbon reservoir corrections for the Mediterranean and Aegean Seas. *Radiocarbon*, *44*(01), 159–166. <https://doi.org/10.1017/S0033822200064766>
- Reitz, A., Thomson, J., de Lange, G. J., Green, D. R. H., Slomp, C. P., & Gebhardt, a. C. (2006). Effects of the Santorini (Thera) eruption on manganese behavior in Holocene sediments of the eastern Mediterranean. *Earth and Planetary Science Letters*, *241*(1–2), 188–201. <http://doi.org/10.1016/j.epsl.2005.10.027>
- Rinna, J., Warning, B., Meyers, P. A., Brumsack, H.-J., & Rullkötter, J. (2002). Combined organic and inorganic geochemical reconstruction of paleodepositional conditions of a Pliocene sapropel from the eastern Mediterranean Sea. *Geochimica et Cosmochimica Acta*, *66*(11), 1969–1986.
- Robinson, A. R., Malanotte-Rizzoli, P., Hecht, A., Michelato, A., Roether, W., Theocharis, A., et al. (1992). General circulation of the Eastern Mediterranean. *Earth-Science Reviews*, *32*, 285–309. [https://doi.org/10.1016/0012-8252\(92\)90002-B](https://doi.org/10.1016/0012-8252(92)90002-B)
- Rohling, E. J. (1991). Shoaling of the Eastern Mediterranean pycnocline due to reduction of excess evaporation: Implications for sapropel formation. *Paleoceanography*, *6*(6), 747–753. <https://doi.org/10.1029/91PA02455>
- Rohling, E. J. (1994). Review and new aspects concerning the formation of eastern Mediterranean sapropels. *Marine Geology*, *122*(1–2), 1–28. [http://doi.org/10.1016/0025-3227\(94\)90202-X](http://doi.org/10.1016/0025-3227(94)90202-X)
- Rohling, E. J., & Gieskes, W. W. C. (1989). Late quaternary changes in Mediterranean intermediate water density and formation rate. *Paleoceanography*, *4*(5), 531–545. <https://doi.org/10.1029/PA004i005p00531>
- Rohling, E. J., Jorissen, F. J., & De Stigter, H. C. (1997). 200 year interruption of Holocene sapropel formation in the Adriatic Sea. *Journal of Micropaleontology*, *16*, 97–108.

- Rohling, E. J., Jorissen, F. J., Grazzini, C. V., & Zachariasse, W. J. (1993). Northern Levantine and Adriatic quaternary planktic foraminifera; reconstruction of paleoenvironmental gradients. *Marine Micropaleontology*, *21*(1–3), 191–218. [http://doi.org/10.1016/0377-8398\(93\)90015-P](http://doi.org/10.1016/0377-8398(93)90015-P)
- Rohling, E. J., Marino, G., & Grant, K. M. (2015). Mediterranean climate and oceanography, and the periodic development of anoxic events (sapropels). *Earth-Science Reviews*, *143*, 62–97. <http://doi.org/10.1016/j.earscirev.2015.01.008>
- Rohling, E. J., & Pälike, H. (2005). Centennial-scale climate cooling with a sudden cold event around 8.200 years ago. *Nature*, *434*(April), 975–979.
- Rohling, E. J., Sprovieri, M., Cane, T., Casford, J. S. L., Cooke, S., Bouloubassi, I., et al. (2004). Reconstructing past planktic foraminiferal habitats using stable isotope data: A case history for Mediterranean sapropel S5. *Marine Micropaleontology*, *50*(1–2), 89–123. [http://doi.org/10.1016/S0377-8398\(03\)00068-9](http://doi.org/10.1016/S0377-8398(03)00068-9)
- Rosignol-Strick, M. (1985). Mediterranean quaternary sapropels, an immediate response of the African monsoon to variation of insolation. *Palaeogeography, Palaeoclimatology, Palaeoecology*, *49*, 237–263.
- Rutten, A., & De Lange, G. J. (2003). Sequential extraction of iron, manganese and related elements in S1 sapropel sediments, eastern Mediterranean. *Palaeogeography, Palaeoclimatology, Palaeoecology*, *190*, 79–101.
- Sachs, J. P., & Repeta, D. J. (1999). Oligotrophy and nitrogen fixation during Eastern Mediterranean Sapropel events. *Science*, *286*(5449), 2485–2488. <http://doi.org/10.1126/science.286.5449.2485>
- Scheiderich, K., Zerkle, A. L., Helz, G. R., Farquhar, J., & Walker, R. J. (2010). Molybdenum isotope, multiple sulfur isotope, and redox-sensitive element behavior in early Pleistocene Mediterranean sapropels. *Chemical Geology*, *279*(3–4), 134–144. <http://doi.org/10.1016/j.chemgeo.2010.10.015>
- Schlitzer, R., Roether, W., Oster, H., Junghans, H.-G., Hausmann, M., Johannsen, H., & Michelato, A. (1991). Chlorofluoromethane and oxygen in the Eastern Mediterranean. *Oceanographic Research Papers*, *38*(12), 1531–1551. [http://doi.org/10.1016/0198-0149\(91\)90088-W](http://doi.org/10.1016/0198-0149(91)90088-W)
- Schmiedl, G., Kuhnt, T., Ehrmann, W., Emeis, K.-C., Hamann, Y., Kotthoff, U., et al. (2010). Climatic forcing of eastern Mediterranean deep-water formation and benthic ecosystems during the past 22 000 years. *Quaternary Science Reviews*, *29*(23–24), 3006–3020. <http://doi.org/10.1016/j.quascirev.2010.07.002>
- Siani, G., Magny, M., Paterne, M., Debret, M., & Fontugne, M. (2013). Paleo hydrology reconstruction and Holocene climate variability in the South Adriatic Sea. *Climate of the Past*, *9*(1), 499–515. <http://doi.org/10.5194/cp-9-499-2013>
- Siani, G., Paterne, M., Arnold, M., Bard, E., Metivier, B., Tisnerat, N., & Bassinot, F. (2000). Radiocarbon Reservoir Ages in the Mediterranean Sea and Black Sea. *Radiocarbon*, *42*(02), 271–280. <https://doi.org/10.1017/S0033822200059075>
- Stratford, K., Williams, R. G., & Myers, P. G. (2000). Impact of the circulation on sapropel formation in the eastern Mediterranean. *Global and Planetary Change*, *14*(2), 683–695.
- Tachikawa, K., Vidal, L.-A., Cornuault, M., Garcia, M., Pothin, A., Sonzogni, C., et al. (2015). Eastern Mediterranean Sea circulation inferred from the conditions of S1 sapropel deposition. *Climate of the Past*, *11*(6), 855–867. <http://doi.org/10.5194/cp-11-855-2015>
- Tesi, T., Asioli, A., Minisini, D., Maselli, V., Dalla Valle, G., Gamberi, F., et al. (2017). Large-scale response of the Eastern Mediterranean thermohaline circulation to African monsoon intensification during sapropel S1 formation. *Quaternary Science Reviews*, *159*, 139–154. <http://doi.org/10.1016/j.quascirev.2017.01.020>
- Theocharis, A. (2009). Variability of the thermohaline properties in the Eastern Mediterranean during the post-EMT period (1995–2008) and SST changes in the Aegean (1985–2008). *CIESM*, (may), 35–40.
- Theocharis, A., & Georgopoulos, D. (1993). Dense water formation over the Samothraki and Limnos Plateaux in the north Aegean Sea (Eastern Mediterranean Sea). *Continental Shelf Research*, *13*(8/9), 919–939. [https://doi.org/10.1016/0278-4343\(93\)90017-R](https://doi.org/10.1016/0278-4343(93)90017-R)
- Theocharis, A., Georgopoulos, D., Lascaratos, A., & Nittis, K. (1993). Water masses and circulation in the central region of the Eastern Mediterranean: Eastern Ionian, South Aegean and Northwest Levantine, 1986–1987. *Deep Sea Research Part II: Topical Studies in Oceanography*, *40*(6), 1121–1142. [http://doi.org/10.1016/0967-0645\(93\)90064-T](http://doi.org/10.1016/0967-0645(93)90064-T)
- Thomson, J., Higgs, N. C., Wilson, T. R. S., Croudace, I. W., De Lange, G. J., & Van Santvoort, P. J. M. (1995). Redistribution and geochemical behaviour of redox-sensitive elements around S1, the most recent eastern Mediterranean sapropel. *Geochimica et Cosmochimica Acta*, *59*(17), 3487–3501.
- Thomson, J., Mercone, D., De Lange, G. J., & Van Santvoort, P. J. M. (1999). Review of recent advances in the interpretation of eastern Mediterranean sapropel S1 from geochemical evidence. *Marine Geology*, *153*(1–4), 77–89. [http://doi.org/10.1016/S0025-3227\(98\)00089-9](http://doi.org/10.1016/S0025-3227(98)00089-9)
- Triantaphyllou, M. V., Gogou, A., Dimiza, M. D., Kostopoulou, S., Parinos, C., Roussakis, G., et al. (2016). Holocene climatic optimum centennial-scale paleoceanography in the NE Aegean (Mediterranean Sea). *Geo-Marine Letters*, *36*(1), 51–66. <http://doi.org/10.1007/s00367-015-0426-2>
- Triantaphyllou, M. V., Ziveri, P., Gogou, A., Marino, G., Lykousis, V., Bouloubassi, I., et al. (2009). Late Glacial-Holocene climate variability at the south-eastern margin of the Aegean Sea. *Marine Geology*, *266*, 182–197.
- Tribovillard, N., Algeo, T. J., Lyons, T., & Riboulleau, A. (2006). Trace metals as paleoredox and paleoproductivity proxies: An update. *Chemical Geology*, *232*(1–2), 12–32. <http://doi.org/10.1016/j.chemgeo.2006.02.012>
- Tzedakis, P. C. (2007). Seven ambiguities in the Mediterranean palaeoenvironmental narrative. *Quaternary Science Reviews*, *26*(17–18), 2042–2066. <http://doi.org/10.1016/j.quascirev.2007.03.014>
- Van Helmond, N. A. G. M., Hennekam, R., Donders, T. H., Bunnik, F. P. M., De Lange, G. J., Brinkhuis, H., & Sangiorgi, F. (2015). Marine productivity leads organic matter preservation in sapropel S1: Palynological evidence from a core east of the Nile River outflow. *Quaternary Science Reviews*, *108*, 130–138. <http://doi.org/10.1016/j.quascirev.2014.11.014>
- Van Os, B. J. H., Lourens, L. J., Hilgen, F. J., De Lange, G. J., & Beaufort, L. (1994). The Formation of Pliocene sapropels and carbonate cycles in the Mediterranean: Diagenesis, dilution, and productivity. *Paleoceanography*, *9*(4), 601–617. <https://doi.org/10.1029/94PA00597>
- Van Os, B. J. H., Middelburg, J. J., & De Lange, G. J. (1991). Possible diagenetic mobilization of barium in sapropelic sediment from the eastern Mediterranean. *Marine Geology*, *100*, 125–136.
- Van Santvoort, P. J. M., De Lange, G. J., Thomson, J., Cussen, H., Wilson, T. R. S., Krom, M. D., & Ströhle, K. (1996). Active post-depositional oxidation of the most recent sapropel (S1) in sediments of the eastern Mediterranean Sea. *Geochimica et Cosmochimica Acta*, *60*(21), 4007–4024.
- Versteegh, G. J. M., Zonneveld, K. A. F., & de Lange, G. J. (2010). Selective aerobic and anaerobic degradation of lipids and palynomorphs in the eastern Mediterranean since the onset of sapropel S1 deposition. *Marine Geology*, *278*, 171–192.
- Von Breyman, M. T., Emeis, K.-C., & Suess, E. (1992). Water depth and diagenetic constraints on the use of barium as a palaeoproductivity indicator. *Geological Society, London, Special Publications*, *64*(1), 273–284. <http://doi.org/10.1144/GSL.SP.1992.064.01.18>

- Warning, B., & Brumsack, H.-J. (2000). Trace metal signatures of eastern Mediterranean sapropels. *Palaeogeography, Palaeoclimatology, Palaeoecology*, 158(3–4), 293–309. [http://doi.org/10.1016/S0031-0182\(00\)00055-9](http://doi.org/10.1016/S0031-0182(00)00055-9)
- Wehausen, R., & Brumsack, H.-J. (1999). Cyclic variations in the chemical composition of eastern Mediterranean Pliocene sediments: A key for understanding sapropel formation. *Marine Geology*, 153(1–4), 161–176. [http://doi.org/10.1016/S0025-3227\(98\)00083-8](http://doi.org/10.1016/S0025-3227(98)00083-8)
- Weldeab, S., Emeis, K.-C., Hemleben, C., Schmiedl, G., & Schulz, H. (2003). Spatial productivity variations during formation of sapropels S5 and S6 in the Mediterranean Sea: Evidence from Ba contents. *Palaeogeography, Palaeoclimatology, Palaeoecology*, 191(2), 169–190. [http://doi.org/10.1016/S0031-0182\(02\)00711-3](http://doi.org/10.1016/S0031-0182(02)00711-3)
- Wilson, T. R. S., Thomson, J., Colley, S., Hydes, D. J., Higgs, N. C., & Sorensen, J. (1985). Early organic diagenesis: The significance of progressive subsurface oxidation fronts in pelagic sediments. *Geochimica et Cosmochimica Acta*, 49, 811–822.
- Wu, J., Filippidi, A., Davies, G. R., & De Lange, G. J. (2018). Riverine supply to the eastern Mediterranean during last interglacial sapropel S5 formation: A basin-wide perspective. *Chemical Geology*, 485(March), 74–89. <http://doi.org/10.1016/j.chemgeo.2018.03.037>
- Wu, J., Liu, Z., Stuut, J. B. W., Zhao, Y., Schirone, A., & De Lange, G. J. (2017). North-African paleodrainage discharges to the Central Mediterranean during the last 18,000 years: A multiproxy characterization. *Quaternary Science Reviews*, 163, 95–113. <http://doi.org/10.1016/j.quascirev.2017.03.015>
- Wu, P., & Haines, K. (1996). Modeling the dispersal of Levantine Intermediate Water and its role in Mediterranean deep water formation. *Journal of Geophysical Research*, 101, 6591–6607.
- Wu, P., Haines, K., & Pinardi, N. (2000). Toward an understanding of deep-water renewal in the eastern Mediterranean. *Journal of Physical Oceanography*, 30, 443–458.
- Wulf, S., Kraml, M., Brauer, A., Keller, J., & Negendank, J. F. W. (2004). Tephrochronology of the 100ka lacustrine sediment record of Lago Grande di Monticchio (southern Italy). *Quaternary International*, 122, 7–30. <http://doi.org/10.1016/j.quaint.2004.01.028>
- Wulf, S., Kraml, M., & Keller, J. (2008). Towards a detailed distal tephrostratigraphy in the Central Mediterranean: The last 20,000 yrs record of Lago Grande di Monticchio. *Journal of Volcanology and Geothermal Research*, 177(1), 118–132. <http://doi.org/10.1016/j.jvolgeores.2007.10.009>
- Zheng, Y., Anderson, R. F., Van Geen, A., & Kuwabara, J. (2000). Authigenic molybdenum formation in marine sediments: A link to pore water sulfide in the Santa Barbara Basin. *Geochimica et Cosmochimica Acta*, 64(24), 4165–4178.
- Ziegler, M., Tuenter, E., & Lourens, L. J. (2010). The precession phase of the boreal summer monsoon as viewed from the eastern Mediterranean (ODP site 968). *Quaternary Science Reviews*, 29(11–12), 1481–1490. <http://doi.org/10.1016/j.quascirev.2010.03.011>